INTERNAL FRICTION IN METALS

Thesis by

Jack Leland Alford

In Partial Fulfillment of the Requirements

For the Degree of

Doctor of Philosophy

California Institute of Technology

Pasadena, California

1950

ACKNOWLEDGEMENTS

The author wishes to express his appreciation to Professor Donald E. Hudson, whose advice and encouragement contributed greatly to this research. Thanks are extended to Dr. P. E. Duwez and his associates at the Jet Propulsion Laboratory for furnishing the porous metals and machining all specimens. Laboratory facilities for this work were provided by the Dynamics Laboratory of the Division of Engineering; this support is gratefully acknowledged.

ABSTRACT

A summary of the current knowledge on the subject of internal friction is presented. An experimental investigation of the variation of specific damping capacity with torsional stress for three metals is described. It is found that the specific damping capacity can be represented by a constant term plus a term linear in stress amplitude. Calculations are made of the effect on specific damping capacity of type of stress and of non-uniform distribution of stress; the calculations are compared with the available experimental data. An expression is proposed to describe the manner in which energy dissipation varies with stress amplitude.

TABLE OF CONTENTS

LIST OF TABLES

LIST OF FIGURES

LIST OF FIGURES (continued)

NOMENCLATURE

A, B	experimental constants
b	width of beam
C	viscous force coefficient
c	constant
D	diffusion constant
d	diffusion distance
E	tensile modulus
e	base of natural logarithms
F	force
f	frequency
G	torsional modulus
H	heat of thermal activation
h	depth of beam
I	moment of inertia
i	$\sqrt{-1}$
K	spring stiffness
l	length of specimen
M	bending moment
Q	figure of merit
R	gas constant
R	outer radius of torsion specimen
r	inner radius of torsion specimen
T	absolute temperature
W	elastic energy
x	longitudinal coordinate of beam
y	vertical coordinate of beam
y	amplitude of vibration
z	horizontal coordinate of beam

α	phase angle
α, β	coefficients of energy dissipation
γ	shear strain
δ	logarithmic decrement
ϵ	normal strain
ξ	bending deflection
ρ	radius
σ	normal stress
τ	shear stress
τ	relaxation time
ψ	specific damping capacity
ω	circular frequency

I. INTRODUCTION

The conventional representation of the relation between stress and strain in a solid material is a curve such as that shown in Fig. 1, obtained from measurements of strain taken as stress is slowly increased. Most such curves are supposed to include an elastic portion, OA, within which the material returns to its original, unstrained state upon removal of the applied stress. For static purposes it is usually adequate to assume that, within this elastic range, the stress and strain are uniquely related, i.e., that both loading and unloading take place along the curve OA. If this were true the net work done in a closed cycle of stress between the limits σ_A and $-\sigma_A$ would be given by --

$$\oint \sigma \cdot d\epsilon = 0 \qquad (1)$$

since stress and strain are in phase throughout the cycle. When the stress σ_A is exceeded, the material will sustain a permanent deformation, OB', upon removal of all stress, as shown in Fig. 3. This higher range of stress is called the plastic range. If the stress be reversed, it is seen that the condition of zero strain corresponds to a finite negative stress. A complete cycle of stress between the limits σ_B and $-\sigma_B$ will trace the loop BB'B''B'''B. In this cycle the strain is not in phase with the stress and an amount of energy is dissipated which is proportional to the to the area of the loop. Because of its similarity to

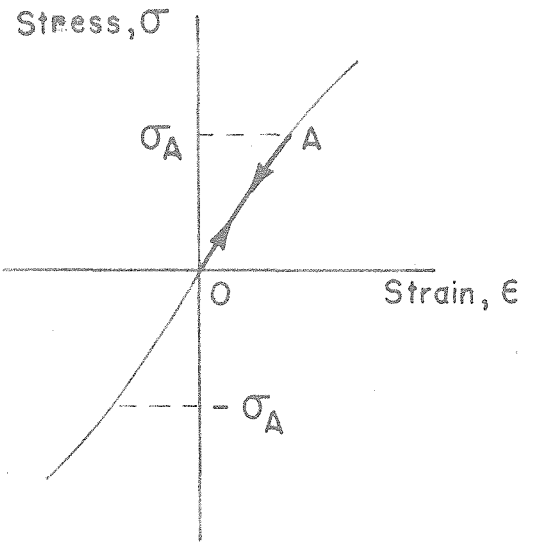

Figure 1. Stress-strain curve of an elastic solid

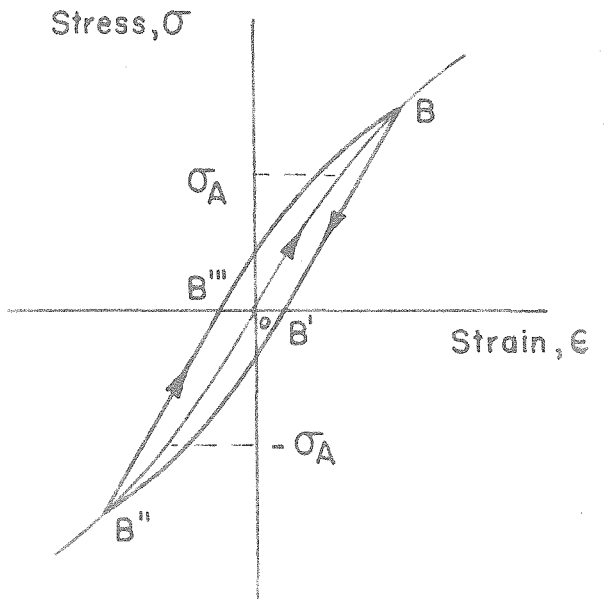

Figure 2. Stress-strain curve of a plastic solid

magnetic hysteresis this phenomenon has been called "elastic hysteresis" (1)*.

The material of a freely-vibrating spring passes through stress-strain cycles of the general type shown in Fig. 2, and the continuous dissipation of vibrational energy is attested to by the gradual decay of the vibration amplitude. Careful experiments, in which energy losses to the supporting and surrounding media have been minimized, show that a small energy loss persists. Since it is unlikely that the motion would continue indefinitely even in the complete absence of external losses, it is assumed that energy is dissipated internally in a cycle of stress no matter how small its amplitude. This reasoning and the fact that measurements of increasing accuracy have usually lowered the experimentally-determined values of the elastic limits of engineering materials have been used to argue that the elastic limit does not exist, i.e., that there is no stress below which a material will not sustain a permanent deformation (2,3).

That this is not necessarily true can be seen by considering the system shown in Fig. 3, a model of visco-elastic solid attributed to Maxwell (4).

The force F is transmitted to the reference frame through a spring K_1 in parallel with the series combination of a spring K_2 and a dashpot C.

---

* The figures appearing in parentheses refer to the references listed at the end of this thesis.

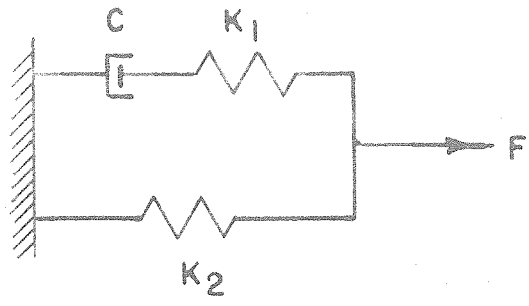

Figure 3. Mechanical model of a visco-elastic solid

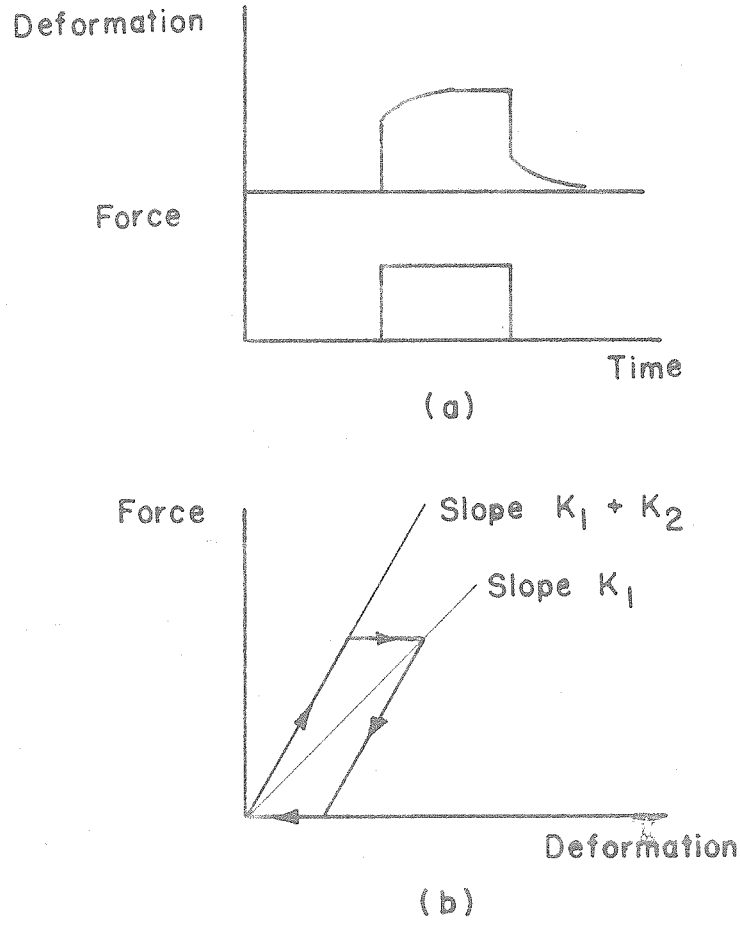

Figure 4. Behavior of the mechanical model

If a constant load be suddenly applied, there will be an instantaneous deformation, followed by an exponential increase of deformation as the force across the dashpot relaxes. Conversely, when the load is released, there will be an instantaneous contraction, followed by a relaxation of the residual strain across the dashpot. Fig. 4a shows this behavior in the force-time and deformation-time planes, and Fig. 4b in the force-deformation plane. If the system be subjected to a force cycle applied infinitely slowly, the force across the dashpot will be completely relaxed at all times and the cycle will traverse the line whose slope is K_1, the "relaxed modulus". Here stress and strain will be in phase and the energy dissipation will be zero. Similarly if the force cycle be applied infinitely rapidly, the force across the dashpot is completely unrelaxed, and the cycle will trace the line whose slope is $(K_1 + K_3)$, the "unrelaxed modulus". Here again stress and strain are in phase and the energy dissipation is zero. At intermediate rates of loading, varying degrees of relaxation will be experienced, stress and strain will be out of phase, and energy will be dissipated in the cycle. It is shown in Appendix A that the energy dissipation will vary with the frequency of the force cycle as shown in Fig. 5, reaching a maximum when the period of the force cycle is equal to the characteristic relaxation time of the model. Here then is a model of a material which cannot sustain a permanent deformation, but which dissipates energy in a

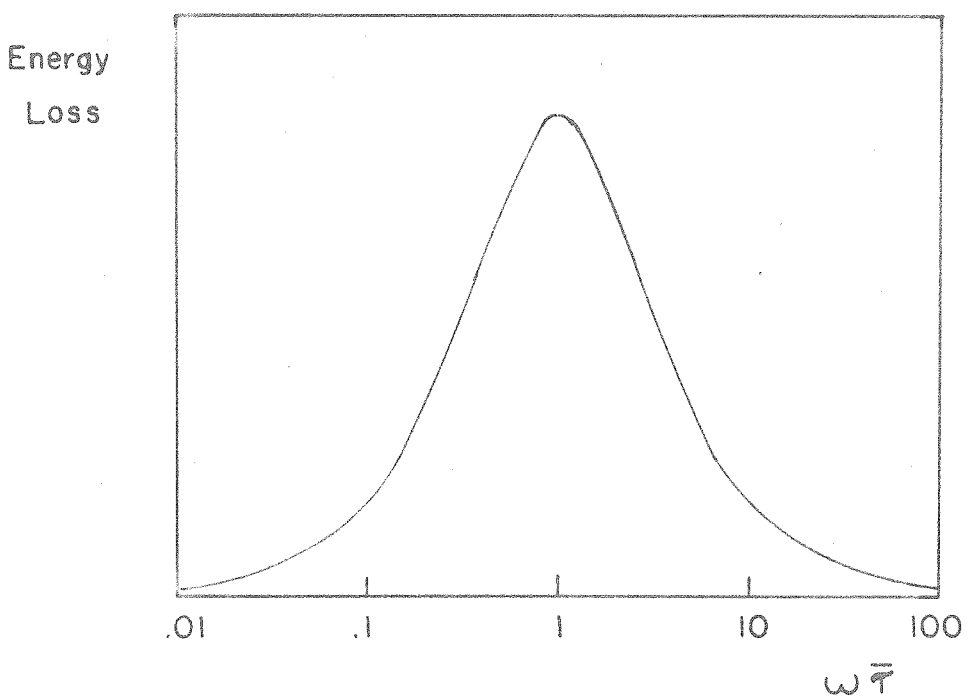

Figure 5. Variation of energy loss with frequency

stress cycle. According to this concept, the permanent or plastic deformation is not essential to energy dissipation; the significant feature is the phase difference between stress and strain during the cycle, the phase difference in this case being associated with a relaxation process.

Since all real materials are known to dissipate energy, it seems likely that no material exists which is elastic in the sense that stress and strain are uniquely related in the pre-plastic range. Zener (5) has called attention to the fact that the essential attribute of the elastic range is the absence of a permanent deformation upon removal of load and that absence of a permanent deformation does not imply a linear relation between stress and strain, nor even a single-valued relation. He defines the property of a solid by virtue of which stress and strain are not uniquely related in the elastic range as "anelasticity". Energy dissipation is but one of the manifestations of anelasticity, of which others are recoverable creep, elastic after-effect, and variation of dynamic modulus.

We have seen that energy may be dissipated within a solid material subjected to cyclic streases by anelastic effects at stress amplitudes within the elastic range, and by plastic flow at stress amplitudes in the plastic range. The sum of these effects is called "internal friction".

B. THE IMPORTANCE OF INTERNAL FRICTION

The importance of damping in limiting the amplitude of a vibrating system is well known, particularly in connection with the design of complex machinery in which the resonant frequencies of one or more members cannot be entirely avoided. Here the presence of damping reduces the magnitude of peak stresses in the machine and thus reduces the likelihood of fatigue failure. Although internal friction was recognized as a source of damping and studied by Lord Kelvin as early as 1865 (6), one of the first attempts to provide engineering data on this property of materials was that of Rowett in 1914 (7). In 1936 Föppl (8) emphasized the importance of internal friction in the vibration of electric transmission lines, turbine blades, and engine crankshafts, asserting that in some cases a material of high damping capacity and low fatigue strength might be superior to one of lower damping and higher fatigue strength.

Internal friction is also important because measurements of it may serve as a non-destructive test of materials. In a qualitative sense this property has been used for hundreds of years to test the soundness of bells; a "dead" tone from the bell indicates abnormally high internal friction, usually the result of a crack or other defect in the metal. Frommer and Murray (9) report the use of quantitative internal friction measurements for the location of internal flaws in

metal bars, and Read, Kitchen, and Fusfeld (10) describe the establishment of a quantitative internal friction criterion for the reuse of artillery shell cases which had been subject to season-cracking. Both of these applications depend upon the fact that material flaws increase internal friction by acting as stress concentrations and increasing stress-sensitive damping, by actual relative motion of surfaces at the defect, or by a combination of the two mechanisms.

Another significance of internal friction, of particular interest to students of the fundamental properties of materials, is the fact that it is extremely sensitive to the structure and past history of the material. This quality makes it a useful tool for observation of structural changes which are difficult to study by direct means. The work of Randall, Rose, and Zener (11) indicates the manner in which internal friction may serve as an index of grain size. Snoek (12) points out how internal friction can be used to show the atomic distribution of carbon and nitrogen in iron. Hanstock (13) shows how measurements of internal friction can be used to determine the extent of precipitation hardening in an aluminum alloy. Several papers by Kê (14, 15, 16, 17) make use of measurements of internal friction and other anelastic effects as evidence of the viscous nature of the grain-boundary material in a polycrystalline metal.

C. THE MEASUREMENT AND SPECIFICATION OF INTERNAL FRICTION

Many methods have been used in the past for the measurement of internal friction; comprehensive reviews of these methods are given in the literature (18, 3, 19). The two most commonly used are the free-vibration method and the forced-vibration method.

In the free-vibration method, the specimen under investigation is given an initial deformation and then allowed to vibrate freely. The gradual decay of the vibration amplitude, resulting from internal friction, is characterized by the logarithmic decrement, which is defined as the natural logarithm of the ratio of successive amplitudes. Referring to Fig. 6, the logarithmic decrement, δ, is given by

$$\delta_n = \ln\left(\frac{y_n + \Delta y_n}{y_n}\right) = \ln\left(1 + \frac{\Delta y_n}{y_n}\right) \qquad (2)$$

Expanding the logarithm in series, we have

$$\delta_n = \frac{\Delta y_n}{y_n} - \frac{1}{2}\left(\frac{\Delta y_n}{y_n}\right)^2 + \frac{1}{3}\left(\frac{\Delta y_n}{y_n}\right)^3 - \cdots\cdots \qquad (3)$$

If $\frac{\Delta y_n}{y_n}$ is very much smaller than unity, as is the case for most metals, the higher powers in the expansion may be neglected and

$$\delta_n = \frac{\Delta y_n}{y_n} \qquad (4)$$

In the ideal case of viscous damping the logarithmic decrement is independent of vibration amplitude and directly proportional to frequency; in real materials, however, at

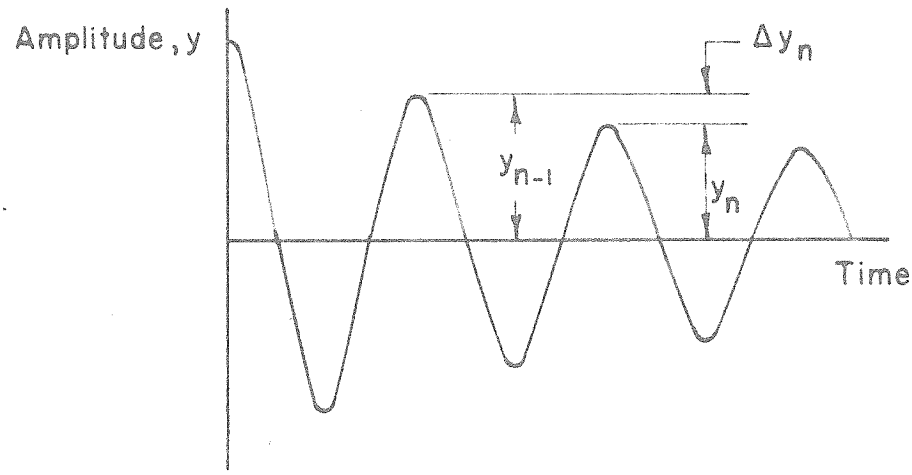

Figure 6. Amplitude-time curve for a free vibration

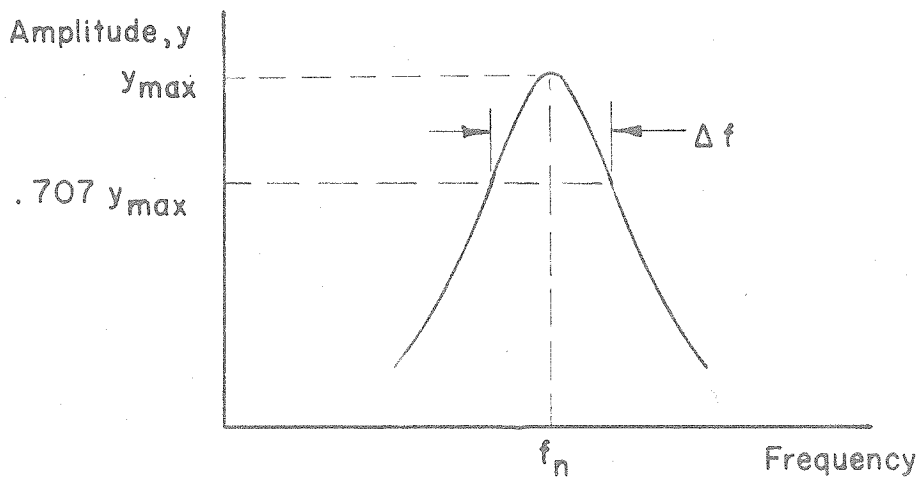

Figure 7. Amplitude-frequency curve for a forced vibration

stress levels of engineering interest, it is a function of stress amplitude and usually does not vary with frequency.

In the forced-vibration method, the specimen is excited by a force of constant magnitude and variable frequency in the vicinity of its resonant frequency. The internal friction is in proportion to the breadth of the amplitude curve thus obtained. Referring to Fig. 7 the internal friction may be specified by the ratio of the breadth of the response curve at a particular amplitude to the resonant frequency, i.e., $\frac{\Delta f}{f_n}$. By analogy with a tuned electrical circuit this quantity is seen to be the reciprocal of the "figure of merit", Q (20).

Another measure of internal friction is the specific damping capacity, ψ, which is defined as the ratio of the energy dissipated in a stress cycle to the maximum elastic strain energy in the cycle. That is,

$$\psi = \frac{\Delta W}{W} \tag{5}$$

It can be readily shown (2, 21, 22) that in a free vibration

$$\psi_n = 2\,\delta_n \tag{6}$$

with an error of less than 1% if the value of δ_n is less than .01.

In Appendix A the internal friction was specified in terms of the tangent of the angle by which strain lags behind stress during the cycle. Zener (23) shows that

$$\tan \alpha = \frac{1}{2\pi} \cdot \psi = Q^{-1} \tag{7}$$

Therefore, we may write in summary

$$\psi = 2\delta = 2\pi Q^{-1} = 2\pi \frac{\Delta f}{f} = 2\pi \tan\alpha \qquad (8)$$

In speaking of internal friction the value of which is independent of stress amplitude either method of measurement is appropriate and these relations may be used interchangeably. When the value of the internal friction is a function of the stress amplitude, however, measurements by the resonance-curve method are meaningless since the stress amplitude varies markedly during the test. For this reason and since the concept of an energy dissipation per cycle is equally valid for free or forced vibration, the specific damping capacity will be used as the measure of internal friction in the following pages.

D. RESULTS OF PREVIOUS INVESTIGATIONS

Until recently the nature of internal friction and the factors which influence its magnitude were imperfectly understood. In 1941 Kimball published a review (18) of the state of knowledge on internal friction up to that time. Tabulation of the results of investigations over the preceding 50 years proved correlation impossible; as Hudson (3) points out, where one investigator reports that copper has twice the specific damping capacity of nickel, another investigator reports just the reverse.

In the light of present-day knowledge this confusion is not surprising; the results of the different investigators are not properly comparable for two reasons. First, the methods and equipment used to measure the internal friction were not the same. Different sizes and forms of specimen, different frequencies and stress amplitudes, different types of stress were used. Second, the materials being tested were not comparable, since composition, structure, mechanical properties and past stress history were not specified.

From the work of many investigators, however, the following facts could be established:

1. At very low stress the internal friction was independent of stress amplitude and dependent on frequency.
2. At higher stress the internal friction was a function of stress amplitude and independent of frequency.

3. Internal friction varied with temperature.
4. No general correlation of internal friction with other material properties had been found.
5. A quantitative treatment, due to Zener, was available for two mechanisms of energy dissipation operative at low stress; these were macroscopic and microscopic thermal flow, which will be described below.

In the ten years since the appearance of Kimball's review tremendous advances have been made in the understanding of internal friction. A recent monograph (33) by Zener provides an outline for a brief description of the current knowledge of anelastic effects.

ANELASTIC EFFECTS

An important mechanism of relaxation in metals is that of thermal diffusion. Raising the temperature of a metal, at constant pressure, causes an increase in volume. Conversely, the sudden application of tension will lower the temperature, causing heat to flow into the metal from its surroundings. As the temperature distribution thus produced relaxes, a small additional extension will take place, with the result that strain lags behind stress and energy is dissipated. This effect was first observed experimentally in the transverse vibration of fine wires by Bennewitz and Rotger (34). The theoretical explanation, due to Zener, Otis, and Nuckolls (35), shows that the mechanism is characterized by a relaxation time which is the time required for heat to flow between regions of extreme temperature. In

the case of the wire, this distance is the diameter and the relaxation time is given by

$$\tau = c \frac{d^2}{D} \qquad (9)$$

where τ = relaxation time

c = constant

d = diameter of wire

D = thermal diffusion constant

When the results were plotted against the dimensionless product $\frac{fd^2}{D}$ a curve of the type shown in Fig. 5 was obtained (f = frequency of vibration).

In the case of transverse vibration, the difference of temperature was caused by the inhomogeneous distribution of stress typical of bending. Reasoning that stress inhomogeneity might also be caused by elastic anisotropy in a polycrystalline metal, Zener (36) developed a theory of damping by intercrystalline thermal currents, which was subsequently demonstrated experimentally by Randall, Rose, and Zener (11). Here the distance between regions of extreme temperature is the average dimension of the grains in the metal; otherwise the theory is similar to that for macroscopic diffusion. Kimball (18) states that damping by thermal diffusion does not occur in torsion experiments since pure shear involves no dilation of the metal lattice. This is true with respect to macroscopic diffusion; however, Entwistle (37) has recently shown experimentally that elastic anisotropy in torsion specimens can bring about the normal stresses necessary to produce a measurable internal friction

due to microscopic thermal diffusion.

As Kimball points out, damping by thermal diffusion is not important in an engineering sense for two reasons: first, although the maximum value of the specific damping capacity associated with transverse thermal currents is of the order of 10^{-2}, an iron reed vibrating at 1000 cycles per second could be only .007 inch thick to realize such an amount of damping; second, the maximum value of the specific damping capacity associated with intercrystalline thermal currents is only of the order of 10^{-4}.

The theory for a second anelastic mechanism was formulated by Gorsky (28), who pointed out that atomic diffusion was subject to the same types of differential equations and boundary conditions as thermal diffusion. The equilibrium state of an unstressed solid solution corresponds to a random distribution of the solute atoms. When stress fluctuations exist within the system, this correspondence no longer holds. Thus, where an increase in the concentration of solute atoms causes an expansion of the lattice, equilibrium conditions under the influence of an impressed dilation will necessitate an increase of concentration. The necessary increase of concentration will occur through atomic diffusion, constituting a relaxation of stress at constant strain. The relaxation time for this process is given by Equation 9, the distance d in this case being the distance between regions of stress inhomogeneity and D the atomic diffusion coefficient. There has been no

demonstration of this mechanism because of experimental difficulties associated with long relaxation times.

The third anelastic mechanism is a result of the magnetoelastic coupling, or magnetostrictive effect as it is sometimes called, in ferromagnetic metals. Even though the average magnetization in a specimen be zero, elementary regions called domains retain finite magnetizations, aligned along the easy directions of magnetization of the lattice. When an external stress is applied, the internal strains shift the directions of easy magnetization, changing the overall magnetization of the specimen. As the magnetization of the specimen changes, the eddy currents which are responsible for the dissipation of energy are set up, of such magnitude that the magnetic flux within the specimen is initially unchanged. Gradual diffusion of magnetic flux takes place, permitting relaxation of the magnetic field strength. The relaxation time for this process is also given by Equation (9), in which now d is the distance over which the flux must diffuse and D the magnetic diffusion constant. Since this mechanism depends upon reorientation of domains, alignment of the domains by a strong external field should suppress it; experiment shows this to be the case. This type of internal friction has been observed by Brown (39); the magnitude of the specific damping capacity associated with it is of the order of .005.

The order-disorder transformation in certain metallic alloys is the source of a fourth anelastic mechanism. This

mechanism depends on the fact that ordering is accompanied by a change in lattice dimensions which depends, at equilibrium conditions, upon the amount by which the temperature is below a critical value. Changes in lattice dimensions by means of impressed strains conversely alter the equilibrium order, and the time delay associated with the establishment of equilibrium leads to anelasticity in the manner described under atomic diffusion. The relaxation time is of the order of 10^7 seconds.

The fifth type of anelastic effect results from the stress-induced preferential distribution of solute atoms in a metallic solid solution. A striking example of this was given by Snoek (13), who found a sharp peak at 30° C and 1/3 cycle per second in the internal friction of annealed iron containing small amounts of carbon and nitrogen. This peak completely disappeared when the iron was treated to remove the carbon and nitrogen; when small traces of carbon and nitrogen were reintroduced, the peak reappeared. Snoek's theory assumes that the carbon and nitrogen atoms occupy interstitial positions at the centers of the cube faces and at the centers of the cube edges of the α-iron lattice. These positions have tetragonal axes of symmetry parallel to the principal axes of the lattice. The interstitial position is closer to those iron atoms which lie along the tetragonal axis; consequently, the presence of solute atoms in these positions will cause greater elastic distortion along this direction.

In an unstressed specimen the interstitial solute atoms will be distributed equally among the positions on the three tetragonal axes. When the tensile stress is applied in the direction of one of the tetragonal axes, the probability that a solute atom will lie in one of the positions along this axis is increased. A finite time is required for the solute atoms to diffuse into these preferred positions and, as a result, strain lags behind stress. This phase lag produces the various anelastic effects, including internal friction. Although specific damping capacities as high as .08 have been observed for this type of internal friction, its engineering applications will probably not be numerous, since the relaxation time for the basic mechanism involved is highly sensitive to temperature.

All of the mechanism listed above were described in connection with homogeneous materials; anelastic effects are also possible in non-homogeneous systems. Imagine an isolated region of viscous character enbedded in an elastic matrix: if a stress be applied to the matrix, the stress across the viscous region will gradually relax. When the stress is removed from the boundary of the matrix, the viscous region will be stressed in a sense negative to that of the original stress. Such a system will exhibit the properties of the simple model of Appendix A.

Possible real counterparts of the viscous regions described above are the slip bands formed in metal crystals by plastic deformation. Internal friction is usually increased

by prior plastic deformation, although investigators are not in agreement as to whether the internal friction thus introduced has the frequency-dependence characteristic of anelasticity.

A more definitely established counterpart of the "viscous regions" is the network of grain boundaries in a polycrystalline metal. Several investigators (30, 31) have observed relative movement between grains extended slowly at high temperature and found no relative movement when similar extensions were rapidly produced at room temperature, indicating that the grain boundaries behave in a viscous manner.

Viscous flow at the grain boundaries during vibration would necessarily dissipate energy, the energy dissipated being proportional to the product of the relative displacement and the shear stress across the boundary. At low temperatures the viscosity would be high and the relative displacement therefore low. At high temperatures the viscosity will be low so that the shear stress across the grain boundary will be relaxed. At intermediate temperatures, where both factors have significant magnitude, the dissipation would be expected to have a maximum value. The existence of this maximum has been observed experimentally in aluminum by Kê (15, 16) at a temperature of approximately 385°C, the frequency being 0.8 cycles per second. The maximum specific damping capacity for this case was 0.55; however the value is very sensitive to temperature and may not prove to be useful in practical application.

The anelastic effects are conveniently summarized by means of a relaxation spectrum, an example of which is shown in Fig. 8.

PLASTIC EFFECTS

The principal contributions to internal friction at large stress amplitudes are characteristically independent of frequency and dependent upon stress amplitude; these effects are usually attributed to plastic deformation. This type of internal friction, although of considerable practical interest in engineering, has not yet been subjected to the intensive fundamental study that the anelastic effects have received.

Since several of the anelastic effects are the result of polycrystalline structure or of ferromagnetism, Read (32, 33, 34) has studied plastic deformation in single crystals of non-ferromagnetic metals. His results demonstrate that the internal friction caused by plastic deformation is amplitude dependent and frequency independent; over a limited initial range he found the internal friction to be a single-valued function of strain amplitude. Overstraining the crystal, however, increased the internal friction measured in subsequent tests. He also found that the increase thus produced could be removed by annealing the specimen. In zinc crystals, in fact, the increase of internal friction produced by cold-work gradually disappears at room temperature, corresponding to the room-temperature resoftening of this metal. Zener, Van Winkle, and Nielsen (35) found that the internal friction of cold-worked brass could be reduced

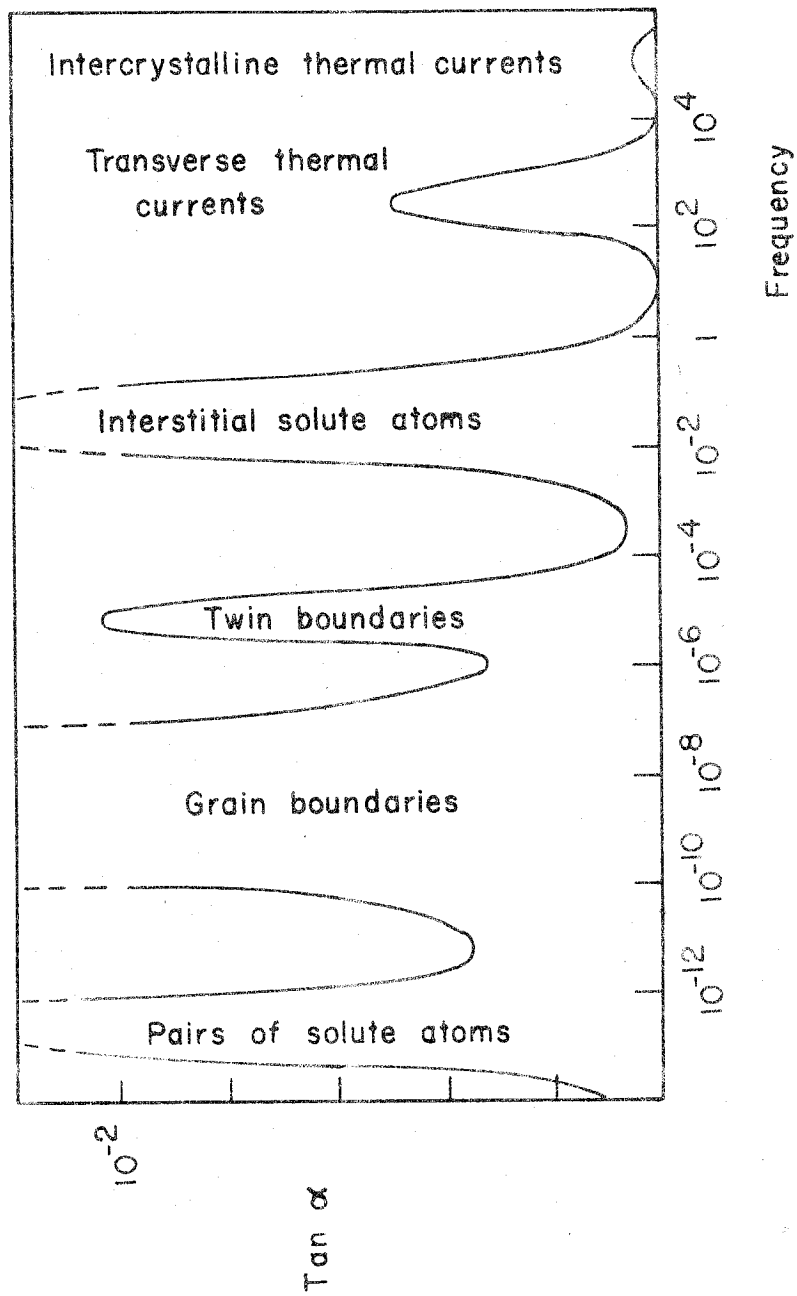

Figure 8. Typical relaxation spectrum (Zener)

by a low-temperature annealing which did not affect the hardness of the metal. Lawson (36) observed that the internal friction of polycrystalline copper reached a maximum and then decreased as the specimen was subjected to increasing amounts of cold-work.

These phenomena have been interpreted qualitatively by Swift and Richardson (37) in terms of dislocation theory, an account of which is given by Seitz and Read (38). According to this interpretation, internal friction arises from the motion of dislocations through the metallic crystals, the strain-independent component of the internal friction being a function of the total number of dislocations initially present in the lattice. It is supposed that not all dislocations can be moved with equal facility, consequently as the stress amplitude increases the number of active dislocations increases. The increase of internal friction after overstrain is the result of the formation of new dislocations; annealing permits these dislocations to diffuse out of the lattice. Since the dislocations which contribute to internal friction are those most readily moved, they can be removed at temperatures too low to affect the more sluggish dislocations associated with strain-hardening. The maximum and subsequent decline in the value of internal friction with extensive cold work can be explained by an increase in the number of dislocations to and beyond a point where they begin to interfere with each other's motion. Several attempts (13, 39) have been made at placing such a theory on a quantitative basis, without complete success.

A number of engineering investigations have been made in the past decade, among which can be mentioned that by Contractor and Thompson (40). These investigators showed that the energy loss in the direct-stylus recording mechanism of the Föppl-Pertz apparatus for the measurement of internal friction was in many cases several times the energy dissipation being measured. This finding is significant since the bulk of the engineering data available prior to this study was obtained by means of the Föppl-Pertz type of apparatus. Hudson (3) made several refinements in the construction of an apparatus for measuring internal friction in torsional vibration and showed that the superposition of a steady axial stress upon the alternating shear stress did not alter the value of the internal friction. Cottell, Entwistle, and Thompson (32) repeated several of the refinements of Hudson and conducted tests in vacuum to measure air damping. As a result of their investigation they concluded that, for a metal of low internal friction such as aluminum, the losses in a Föppl-Pertz apparatus might amount to 500 times the intrinsic energy dissipation in the specimen.

Schabtach and Fehr (41), using specimens in the form of tuning forks, recorded data for a group of turbine alloys at high stresses and at both room and elevated temperatures. Robertson and Yorgiadis (3), using a novel method developed by Lazan (31), made direct measurements of energy dissipation as a function of stress amplitude for a variety of materials; they concluded that the energy dissipation, which

they attributed to plastic effects, is proportional to the third power of the stress amplitude.

The present writer (42) investigated the internal friction of a porous metal produced by powder metallurgy; the specific damping capacity and its variation with stress were found to be not unlike those of conventional metals.

Two papers have been published regarding the quantitative use of internal friction data in engineering design calculations. Gemant (43) made an approximate calculation for the vibration of a turbine blade, based upon the assumption that the specific damping capacity varies as the square of the maximum stress. Since the experimental evidence for such a variation is meager, the consequences of other assumed variations are of interest. Marin and Stulen (44), in an attempt to evaluate the relative importance of internal friction and fatigue strength in the design of resonant members, calculated the energy dissipation in a vibrating cantilever beam. Their calculation was made on the basis of static beam theory and, since no experimental confirmation is available, the value of the result is questionable.

The various types of internal friction are summarized in Figure 9, together with such information as might assist in isolating them experimentally.

TYPE	MECHANISM	Frequency Variation	Temperature Variation	Relaxation Time	Maximum γ
ANELASTIC	Thermal diffusion	$\gamma \sim \frac{\omega\tau}{1+(\omega\tau)^2}$	None		
	(a) macroscopic			10^{-1}	10^{-2}
	(b) microscopic			10^{-5}	10^{-4}
	Magnetic diffusion			$10^{-1} - 10^{-4}$	10^{-2}
	Atomic diffusion		$\tau \sim e^{H/RT}$	10^{7}	
	Order-disorder transformation			10^{7}	10^{-2}
	Preferential distribution			10^{2}	10^{-1}
	Grain boundary slip			10^{9}	10^{-1}
PLASTIC	Plastic flow	None	Indefinite	None	10^{-1}

Figure 9. Summary of internal friction types

II THE PRESENT INVESTIGATION

A. OBJECTIVES

The summary of the literature given in the preceding section indicates that knowledge of internal friction is still not in a state in which it can be put to quantitative use by the design engineer or the stress analyst. Even such meager data as are available are of largely comparative value for lack of a quantitative treatment. Ideally, it would be desirable to have reliable data, obtained by means of a standard test, which could be applied to a variety of situations such as are to be found in modern mechanical and structural designs. For this purpose it would be necessary to know the variation of internal friction with the type of stress, with the magnitude of stress, and with the distribution of stress. In order to isolate these effects it would be desirable to maintain close control over such variables as composition, structure, and past history of the materials used in the experiments.

With the general objective of rendering the damping in an engineering design calculable, it was decided to investigate these three aspects of the problem. A secondary objective was to extend the previous study (43) made by the writer on the internal friction of porous metals.

The objectives of this investigation may be summarized as:

1. To study experimentally the relation between

internal friction and stress amplitude in two metals in the range of medium stress.

3. To study the effect on internal friction of stress distribution by comparing results from solid and hollow torsional specimens of identical material.

3. To study the effect on internal friction of the type of stress by comparing results from flexural and torsional vibration of specimens of identical material.

4. To study the internal friction of a porous metal.

B. EQUIPMENT AND METHOD OF TESTS

The apparatus used for the measurements of specific damping capacity in torsional vibration was that developed by Hudson (3). The system is represented in Figure 10; basically it consists of a torsional pendulum and an optical recording system. The specimen, of which Figure 11 is a typical example, forms the torsion member. It is attached by means of threaded collet chucks to an inertia member at its lower end and to a rigidly mounted frame at its upper end. A permanent record of the vibration amplitude is produced by a light beam focused on a moving strip of photographic paper, the displacement of the light beam being proportional to the angle of twist of the specimen.

The method of testing was to give the pendulum an initial deflection by means of armatures attached to the inertia member and deflection coils attached to the frame, and to record the decay of amplitude of the free torsional vibration produced by opening the deflection coil circuit. Minor modifications were made to the original apparatus to make possible larger torques and deflections without mechanical interference between armature and coil structure. Calibration of the records was direct since the record amplitude is equal to twice the product of the angular deflection of the specimen and the length of the optical lever.

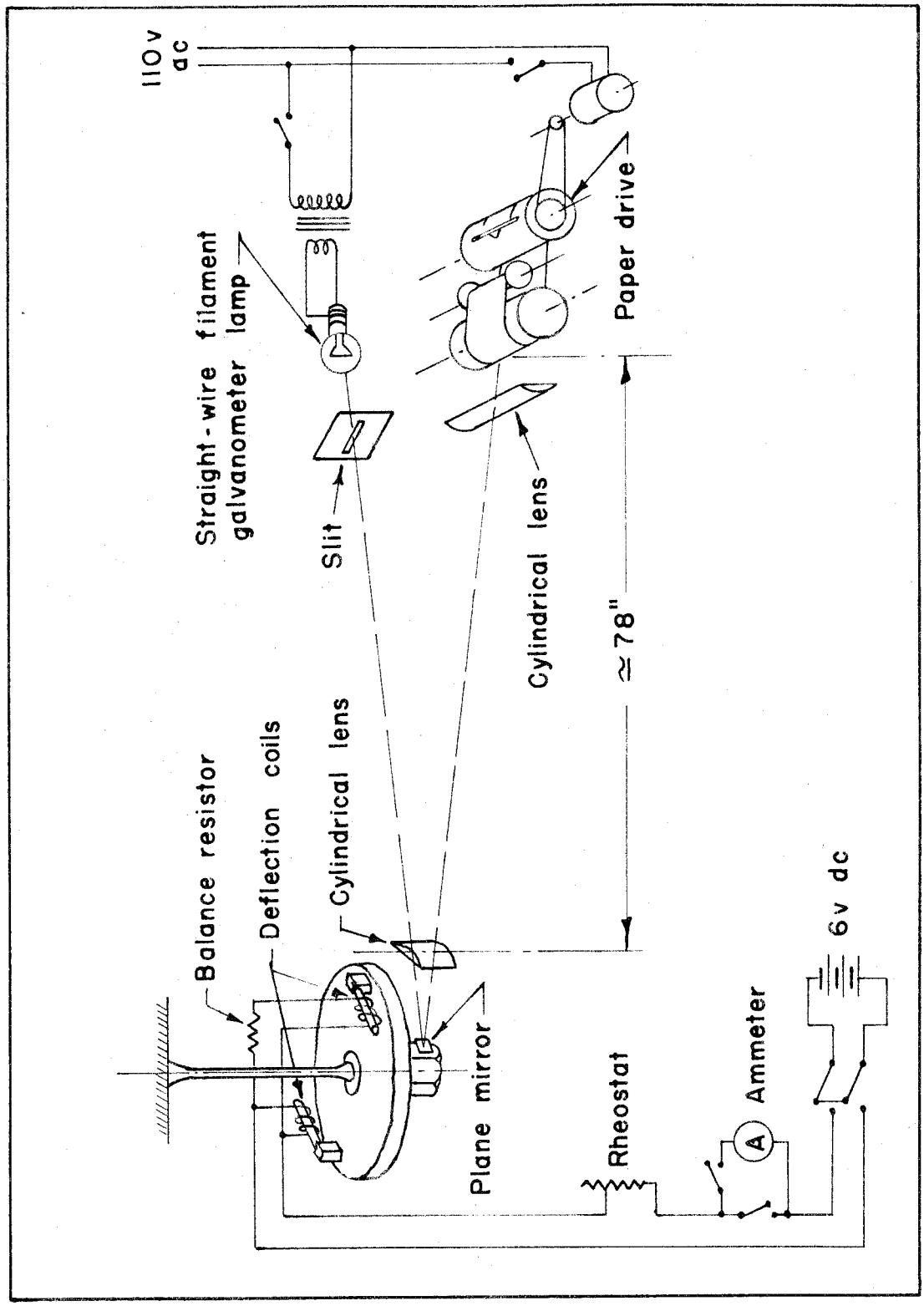

Figure 10. Schematic diagram of torsion apparatus (Hudson)

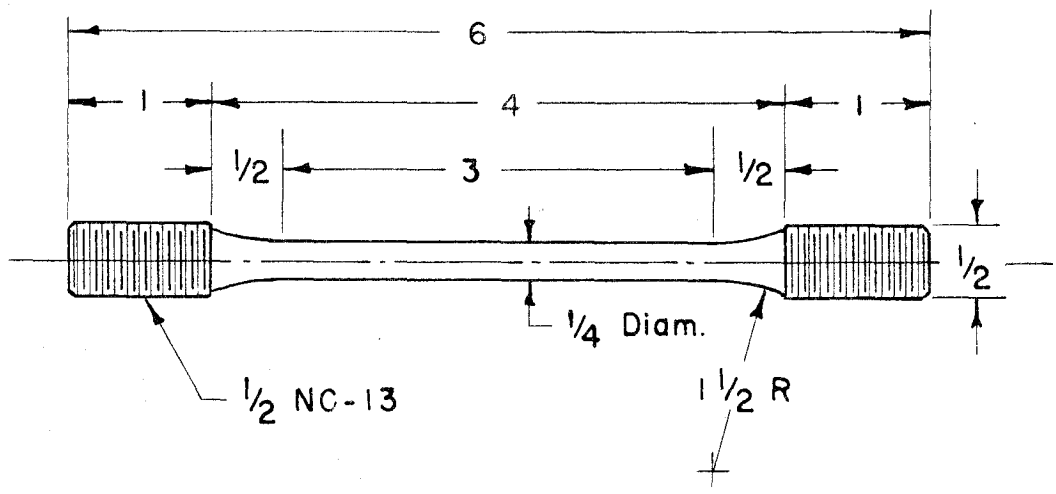

Figure 11. Torsional specimen

Calculation of Specific Damping Capacity: Combining Equations 4 and 6, we find that the specific damping can be approximated by

$$\psi = 2 \frac{\Delta y_n}{y_n} \qquad (10)$$

The error of approximation is less than 1 percent for all measurements reported in this thesis. Since in every case the amplitude decrement, Δy_n, between successive cycles was too small for accurate measurement, the average decrement per cycle over a group of 50 cycles was used. The experimental records were counted off into groups of 50 cycles, and the amplitudes of every fiftieth cycle were measured. From these data the average decrement per cycle could be obtained. The amplitude in the expression of Equation 10 was taken as the mean amplitude of the group. A sample calculation is shown on page 34.

SAMPLE CALCULATION SHEET

Record No. 17 Specimen No. 16

Cycle No.	Amplitude 10^{-3} in.	Difference 10^{-3} in.	Mean Ampl. 10^{-3} in.	γ	τ lbs/in^2
0	3071				
		437	2853	.00618	1390
50	2637				
		361	2454	.00589	1195
100	2273				
		279	2134	.00523	1040
150	1994				
		243	1873	.00519	913
200	1751				
		201	1651	.00486	805
250	1550				
		170	1465	.00464	713
300	1380				
		142	1309	.00435	635
350	1238				
		121	1178	.00411	573
400	1117				
		113	1061	.00433	517
450	1005				
		91	960	.00379	467
500	914				

C. THE MATERIALS TESTED

In order that comparisons might be made, two metals were selected which have been investigated in recent studies. Both Schabtach and Fehr (41) and Robertson and Yorgiadis (3) report experiments on a low-carbon and a chromium-molybdenum steel; for this reason SAE 1022 and SAE x-4130 steels were chosen. Complete physical and chemical properties of these materials as tested are given in Table I; photomicrographs showing their micro-structures constitute Figure 12.

The porous metal tested was an 80% iron-20% nickel alloy, produced by mixing the powdered metals with ammonium bicarbonate as a porosity-producing agent. The mixed powders were compacted under a pressure of 80,000 lbs/sq.in. and sintered at 2400° F. The average porosities of the individual specimens are given in Table II.

TABLE I

PHYSICAL AND CHEMICAL PROPERTIES OF STEEL SPECIMENS

PHYSICAL PROPERTIES

	SAE 1023	SAE x-4130
Ultimate tensile strength	90,000 lb/in^2	90,500 lb/in^2
Yield strength	56,500 lb/in^2	86,000 lb/in^2
Elongation in 1 1/4 in.	34%	18%
Reduction of area	64%	59%
Rockwell hardness	B81	B84

NOTE: All specimens were stress-relieved 1 hour at 600° F after machining.

CHEMICAL COMPOSITION

	SAE 1023	SAE x-4130
Carbon	0.16%	0.32%
Manganese	0.92%	0.58%
Phosphorus	0.021%	0.020%
Sulphur	0.033%	0.021%
Silicon		0.32%
Chromium		1.04%
Nickel		0.26%
Molybdenum		0.26%
Copper		0.16%

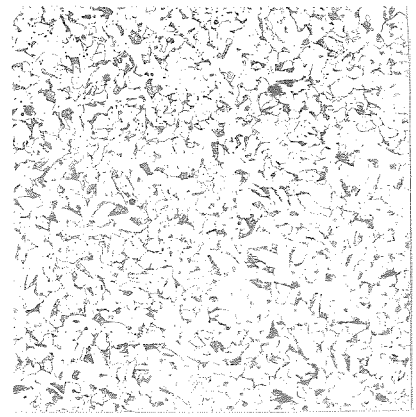

X 100 Nital etch

SAE 1022

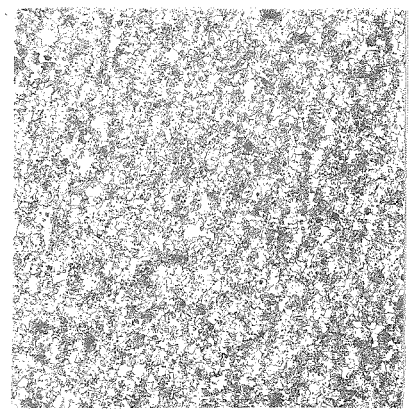

X 100 Nital etch

SAE X-4130

Figure 12. Microstructure of steel specimens

TABLE II

POROSITY OF IRON-NICKEL SPECIMENS

Specimen No.	Percent Ammonium Bicarbonate added	Percent Porosity
10	0	18.3
11	0	17.3
12	0	16.0
13	5	39.3
14	5	38.7
15	5	38.5
16	10	39.7
17	10	39.1
18	10	37.6

III. RESULTS OF THE EXPERIMENTS

A. DESCRIPTION OF THE RESULTS

The results of the experiments are presented in Figures 13 through 19. Figures 13 and 14 are plots of specific damping capacity versus maximum torsional stress for solid specimens of SAE 1032 and SAE x-4130 respectively. Corresponding results for the hollow cylindrical specimens are given in Figures 15 and 16. Figures 17, 18, and 19 represent the results for the porous metals, each figure pertaining to an alloy of different porosity.

Inspection of these figures shows that the data appear to disperse about lines of positive x-intercept and positive slope. The data for groups of three steel specimens of solid cross-section lie close enough together that they may be represented by a common line. With a single exception, referred to below, the data for repeated tests on the same specimen may be represented by a common line. In the case of the porous metals the differences between specimens of the same nominal porosity are great enough that the results for these specimens are treated separately.

The data for Specimen 13, Figure 18, appear to define two lines having the same intercept but different slopes. The results of the first test at low stresses have a low slope while the results of the second test, at higher stresses, have a greater slope.

Mean lines were fitted to the data by the method of least squares; the calculated slopes and intercept are tabulated

in Table III. These values are used in subsequent numerical calculations based upon the experimental results.

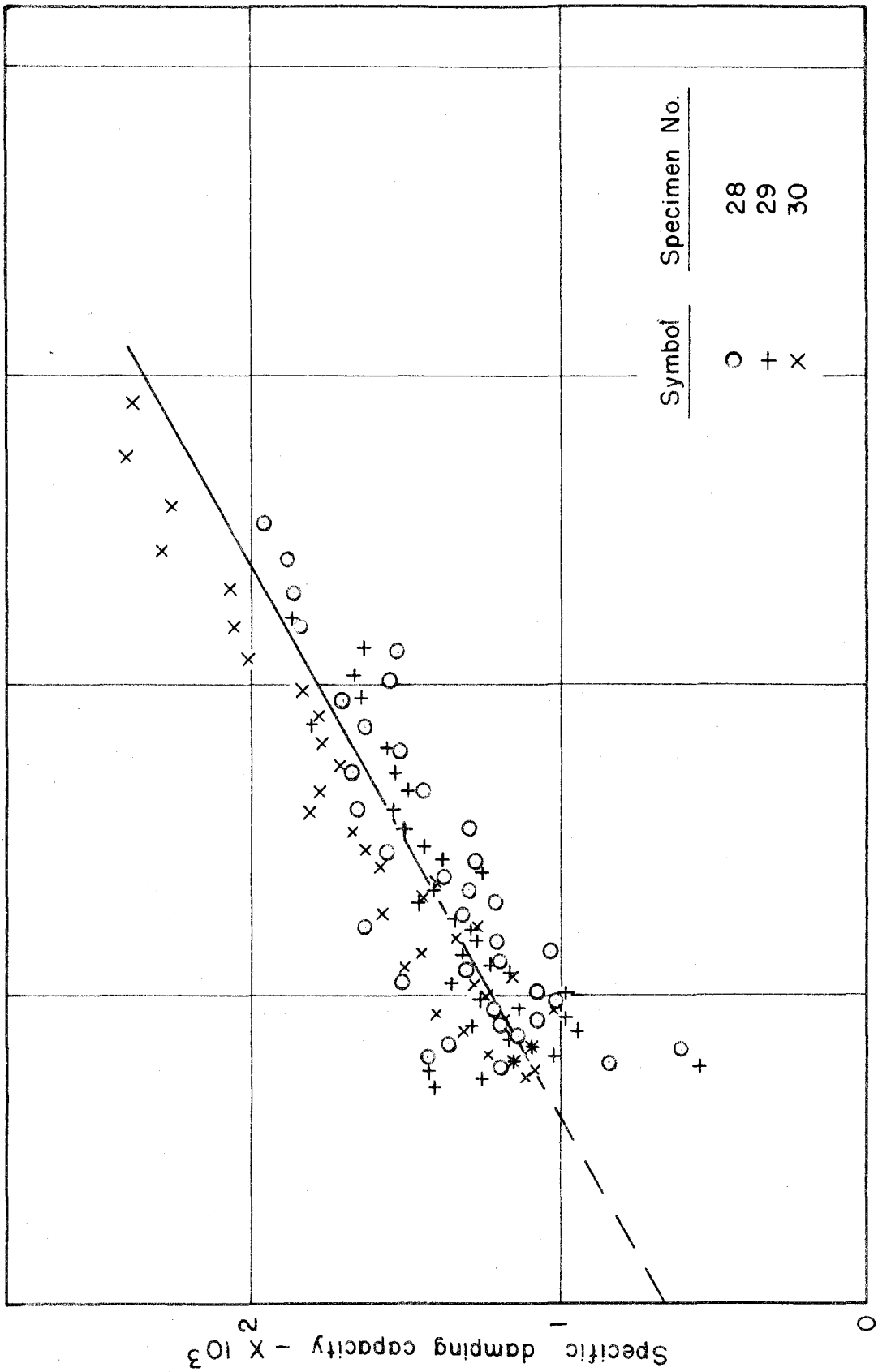

Figure 13. Specific damping capacity vs. maximum shear stress, SAE 1022

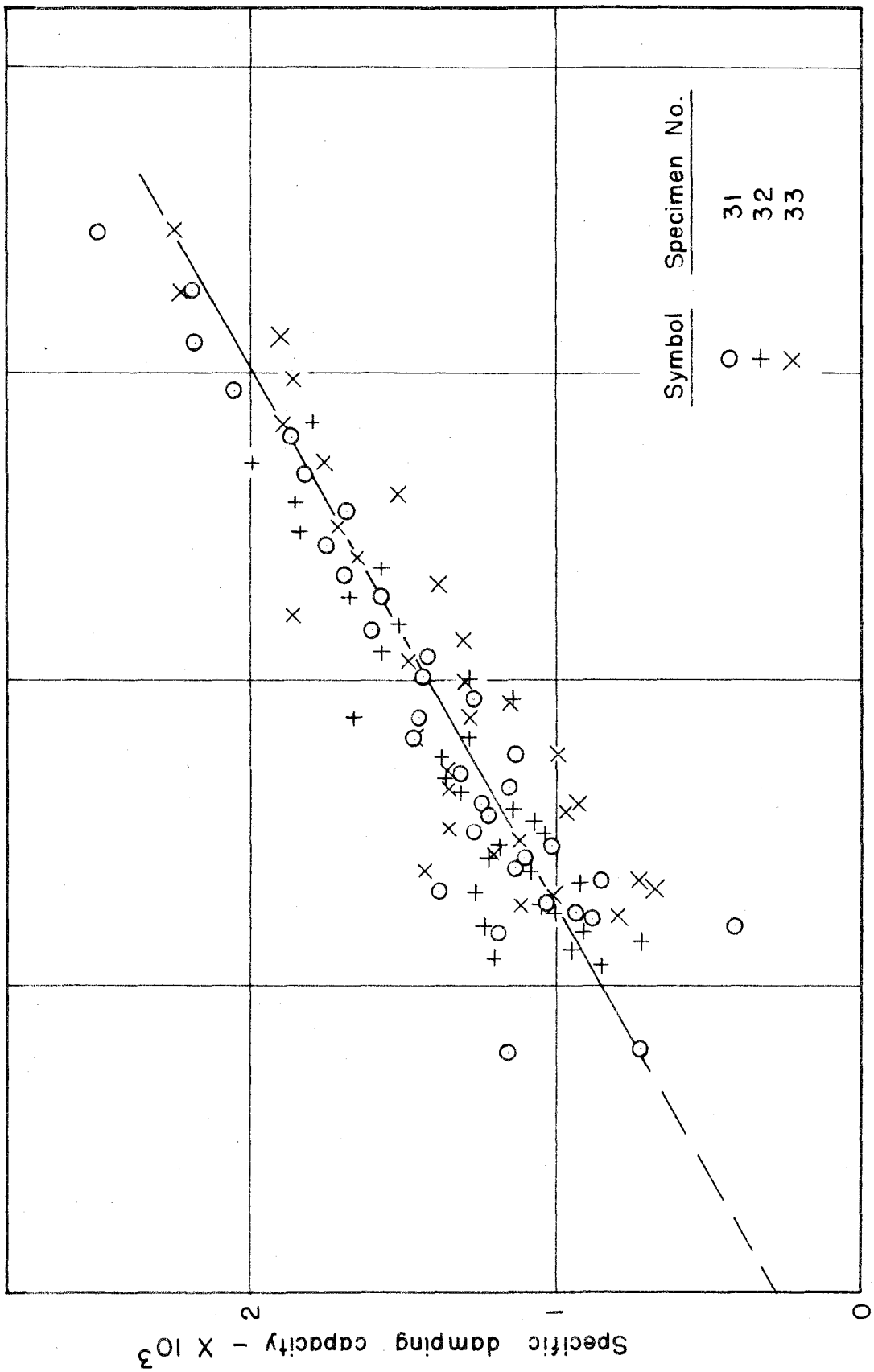

Figure 14. Specific damping capacity vs. maximum shear stress, SAE X-4130

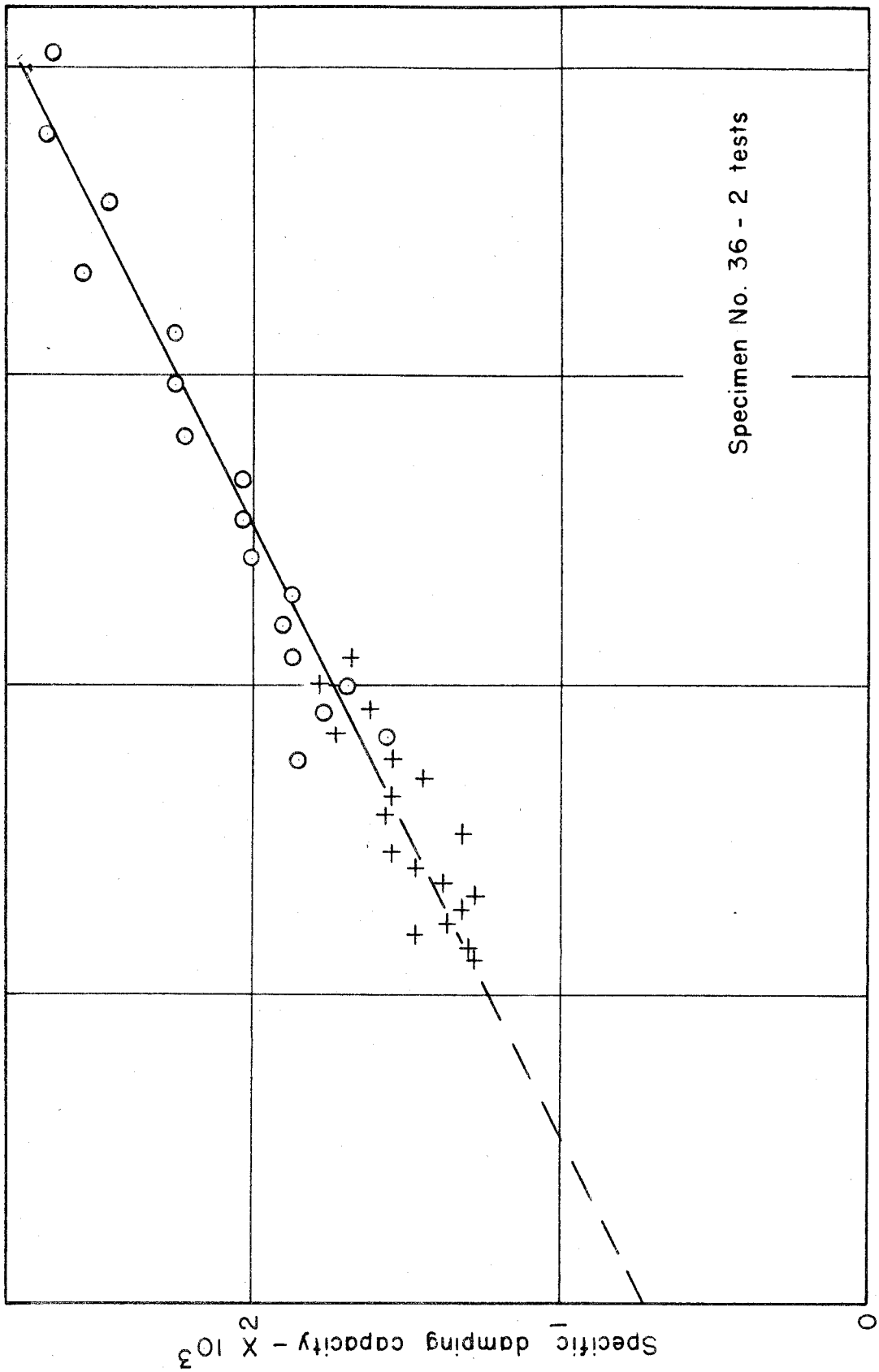

Figure 15. Specific damping capacity vs. maximum shear stress, SAE 1022 (hollow specimen)

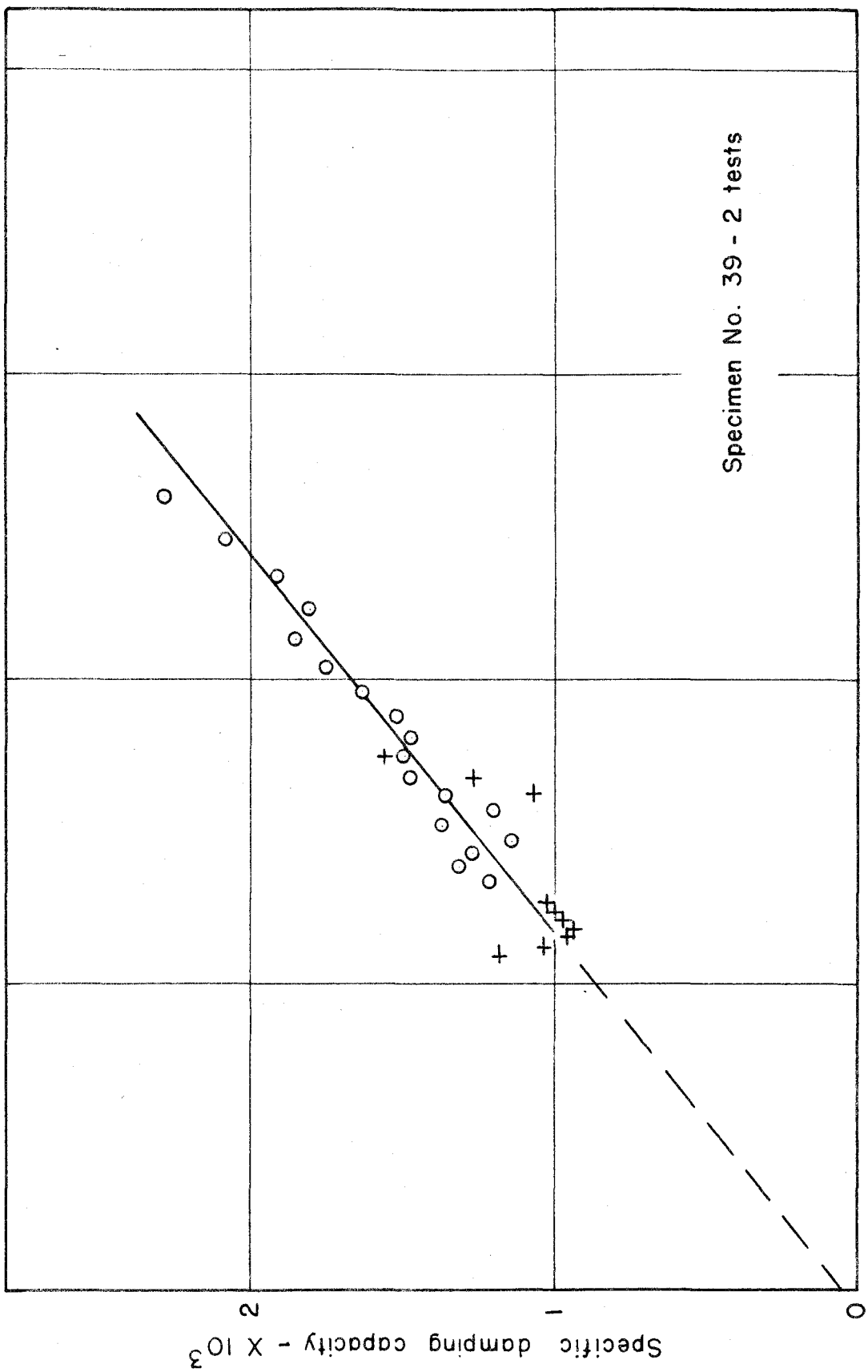

Figure 16. Specific damping capacity vs. maximum shear stress, SAE X-4130 (hollow specimen)

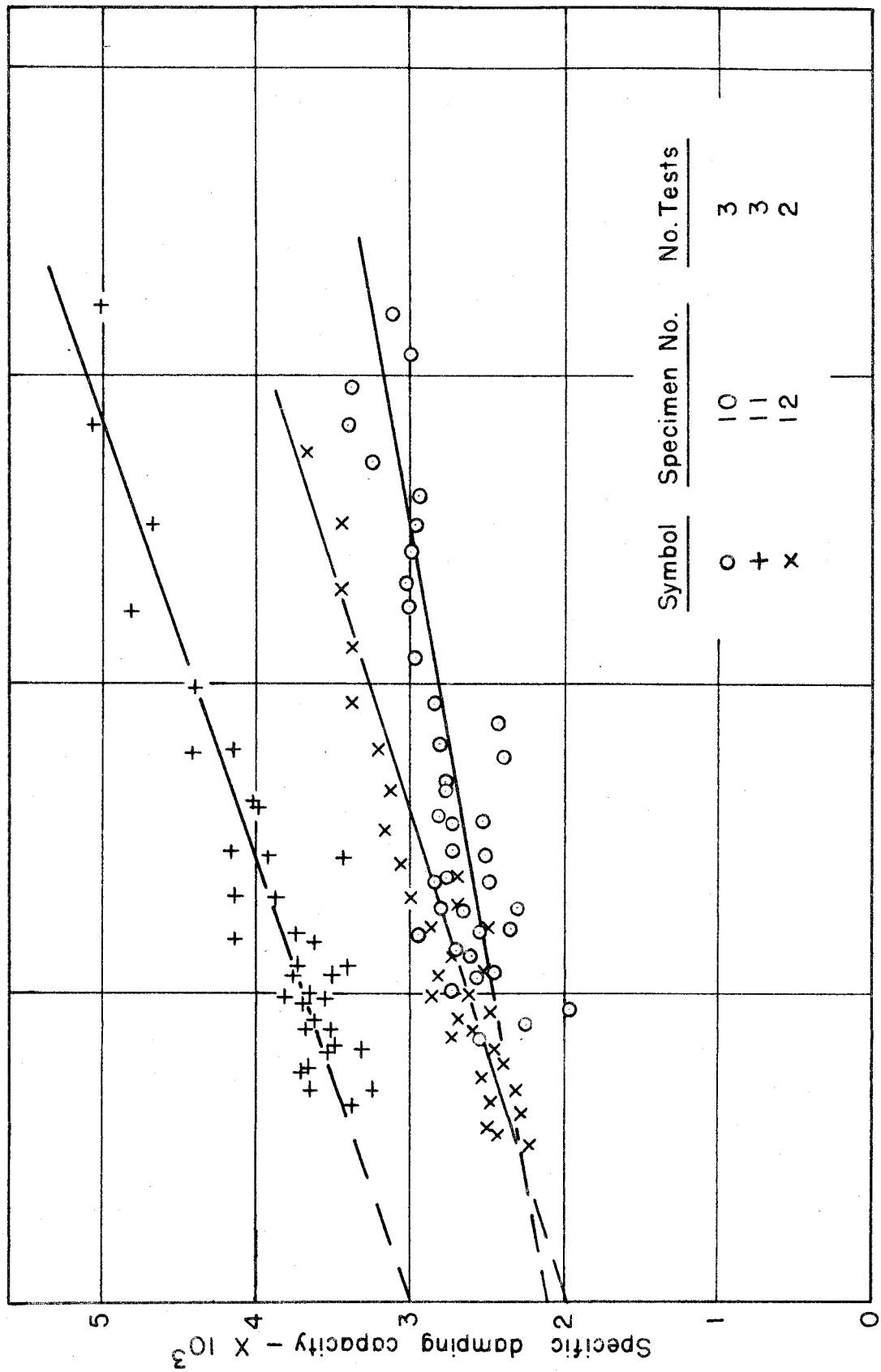

Figure 17. Specific damping capacity vs. maximum shear stress, Iron – Nickel alloy (17% porosity)

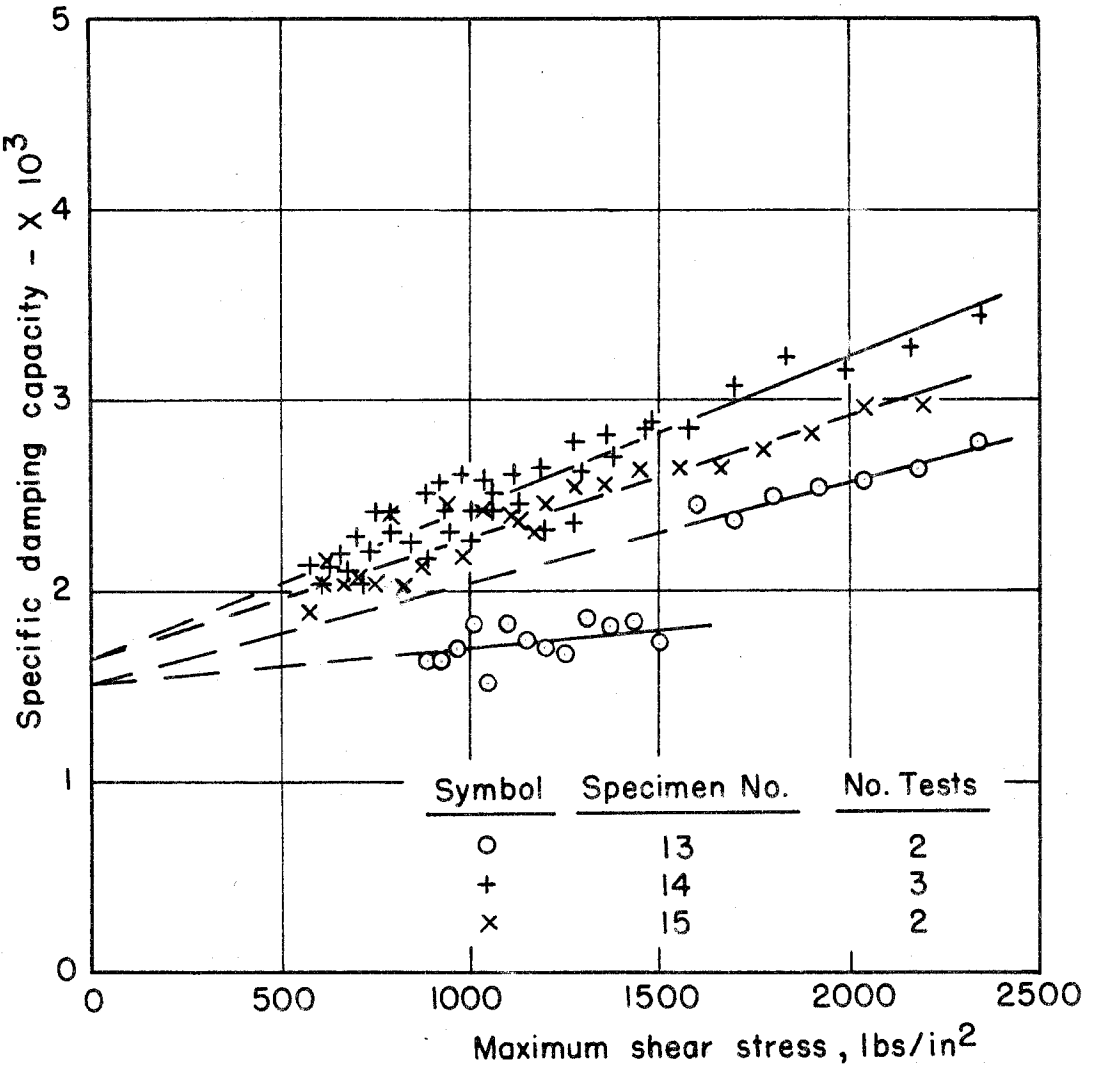

Figure 18. Specific damping capacity vs. maximum shear stress, Iron-Nickel alloy (29% porosity)

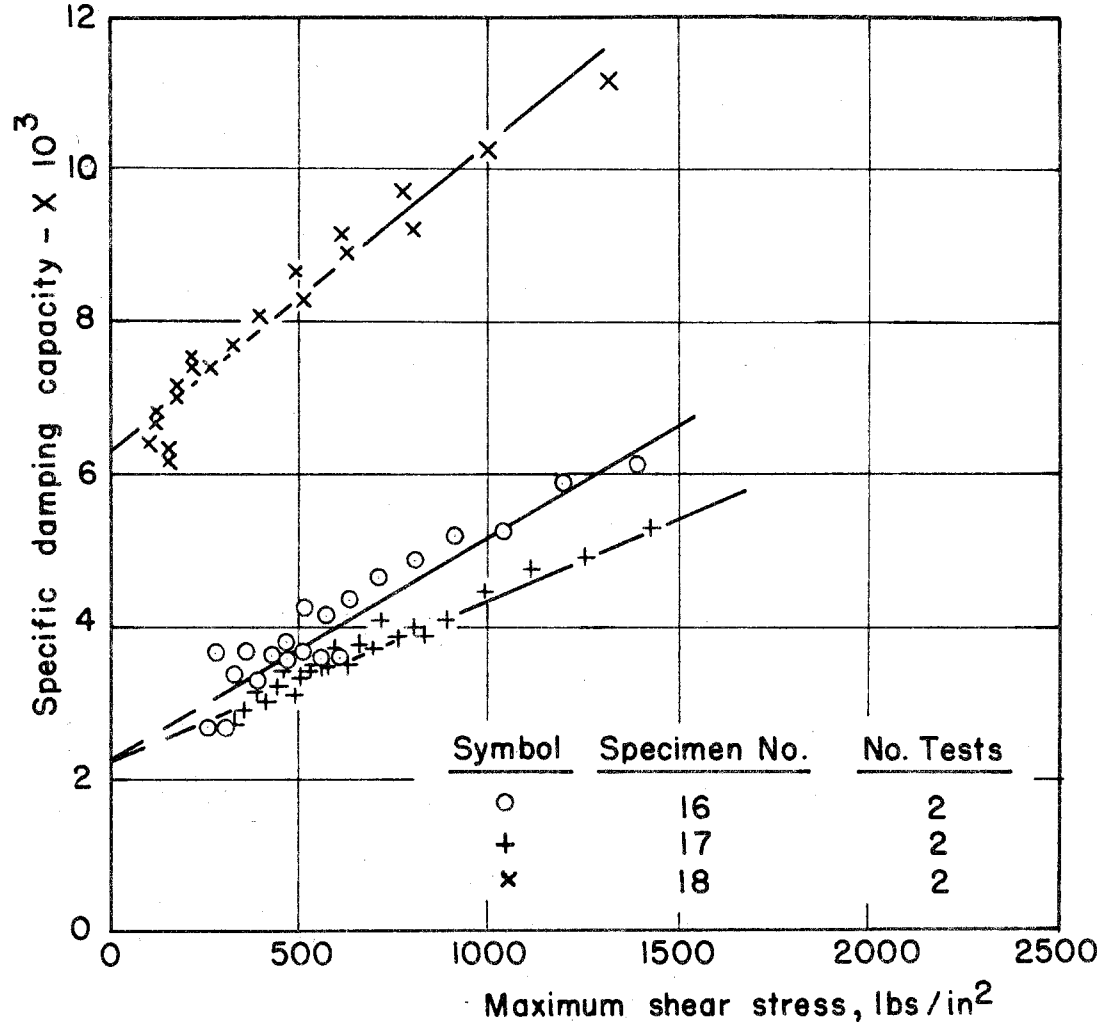

Figure 19. Specific damping capacity vs. maximum shear stress, Iron-Nickel alloy (39% porosity)

TABLE III

SLOPES AND INTERCEPTS OF MEAN LINES IN FIGURES 14 THROUGH 20

Figure No.	Specimen No.	$\psi_0 \times 10^3$	$\frac{d\psi}{dT} \times 10^6$
13	28, 29, 30	0.65	0.56
14	31, 32, 33	0.28	0.57
15	36	0.73	0.51
16	39	0.05	0.81
17	10	2.1	0.36
	11	3.0	0.70
	12	2.0	0.64
18	13	1.5	* { 0.30 0.50
	14	1.6	0.78
	15	1.6	0.64
19	16	2.3	2.9
	17	2.2	2.2
	18	6.2	4.1

* See comment in text.

B. ACCURACY OF THE RESULTS

In discussing the accuracy of the experimental results, it is necessary to distinguish between errors caused by losses of energy other than internal friction and errors involved in measuring from the records and calculation of the results. Extraneous losses of energy may take the form of losses to the specimen supports, losses to the surrounding air, or losses in the recording system.

In the tests, the specimen was tightly clamped at either end in threaded collet chucks. It was demonstrated by Hudson(3) that the torque required to slip the specimen in the chuck was many times that developed by the apparatus. The upper chuck was drawn into a heavy frame which in turn was solidly bolted to a massive concrete pier; the amplitude of motion of the foundation and consequently the energy lost to the foundation are believed to be negligible. This view is supported by the fact that Hudson made consistent measurements of specific damping capacity with this apparatus as low as 3×10^{-4}.

Cottell, Entwistle, and Thompson (33) have investigated the air damping in an apparatus of this type with the aid of a vacuum chamber. Their results indicate that the specific damping capacity associated with air friction for the size and frequency of the present machine will be about 4×10^{-5}, a completely negligible quantity in comparison to the values reported in this thesis.

Since the recording system employs a beam of reflected light, no damping is expected in this phase of the tests. Although the armatures used to give the specimen its initial deflection undoubtedly retained some permanent magnetisation, the solenoid coil circuit was open during the test so that energy was not dissipated in generating currents.

The records of the torsional tests were measured with a comparator graduated in units of 10^{-3} inch; readings were estimated to .5 x 10^{-3} inch. Trial showed that the maximum amplitude on the photographic record could be located within ± .5 x 10^{-3} inch. Since two such measurements must be made for the determination of each record double-amplitude and since each decrement is the difference between successive double-amplitudes, the error of the measured decrements is of the order of ± 2 x 10^{-3} inch. The error in the calculated value of specific damping capacity thus varies with the size of the decrement. When decrements of the order of 100 x 10^{-3} inch are involved, the error will be ± 2 percent; when decrements of the order of 10 x 10^{-3} inch are involved the error will be ± 20 percent.

As a check on the preceding estimate, repeated measurements were made on two records to determine the reproducibility of the results calculated from a given photographic record. Two records were chosen, one in which the specific damping capacities were approximately 2 x 10^{-3} and another in which they were in the neighborhood of .5 x 10^{-3}. It was

found that in the first record the mean difference of the values calculated in successive trials was 1×10^{-4}; in the second record the mean difference was 3×10^{-4}. Since these values represent larger percent errors than those estimated above, they will be considered the errors involved in calculation from the photographic records.

The absolute error in the calculated stress values is no less than that involved in the assumption that the tensile modulus for steel is 30×10^6 lb/in^2; all stress calculations are based on this figure. Torsional stresses are subject to an additional maximum error of $\pm$ 1 percent due to unavoidable tolerances in the measurement of calibration lengths.

The relative error in stress values will be somewhat less, corresponding to the error of record double-amplitude measurement. The maximum relative error for torsional stress is therefore less than 0.5 percent.

IV. THE PREDICTION OF SPECIFIC DAMPING CAPACITY

In the Introduction it was emphasized that the anelastic behaviour of solids was characterized by a phase difference between stress and strain. If the angle by which strain lags stress is α, the energy dissipated by a unit volume in a closed cycle of stress can be found in the following manner.

Let

$$\tau = \tau_0 \sin(\omega t + \alpha)$$
$$\gamma = \gamma_0 \sin \omega t \qquad (11)$$

Substituting Equations 11 in Equation 1, we find the energy dissipated per cycle

$$\Delta W = \int \tau_0 \sin(\omega t + \alpha)\, d(\gamma_0 \sin \omega t) \qquad (12)$$

Performing the integration, we have

$$\Delta W = \pi \tau_0 \gamma_0 \sin\alpha \qquad (13)$$

Since the anelastic effect is small, it is still approximately true to say that stress is proportional to strain. Combining Equation 13 with Hooke's Law, we obtain

$$\Delta W = \frac{\pi \sin\alpha}{G} \tau_0^2 \qquad (14)$$

That is, the energy dissipated is proportional to the sine of the phase angle and to the square of the maximum stress. The specific damping capacity for the unit volume is found by dividing Equation 14 by the elastic energy density, $\tau_0^2/2G$,

$$\psi = 2\pi \sin\alpha \qquad (15)$$

(Note that Equation 15 is equivalent to Equation 8 since $\sin\alpha \simeq \tan\alpha$ for small α.)

Equation 15 serves to make clear what is meant by "internal friction independent of stress amplitude". The equivalent statement, that energy dissipation is proportional to the square of the stress amplitude, is perhaps more descriptive.

It is shown in Appendix A that $\tan\alpha$ is a function of the frequency of vibration; consequently Equation 15 is not adequate to describe the type of internal friction most important in engineering applications. Many investigators have suggested that for plastic effects the energy dissipation per unit volume per cycle varies according to a law of the form

$$\Delta W = c\,\tau^n \qquad (16)$$

Kimball and Lovell (45) gave 3 as the value of the exponent; Lewis (46) proposed the value of 2.3; Rowett (7) and Robertson and Yorgiadis (3) found that their data were best described by an exponent of 3.

In order to investigate the applicability of such a law, we shall calculate the specific damping capacity of a torsion specimen subject to Equation 16. Consider a specimen of radius R and length l, vibrating as in the experiments described above. The total energy dissipated is obtained by integrating Equation 16 over the volume of the specimen:

$$\Sigma(\Delta W) = \int_0^R c\tau^n \cdot 2\pi l \rho\, d\rho$$

Noting that $\tau = \rho/R \cdot \tau_m$ and performing the integration, the above expression becomes:

$$\Sigma(\Delta W) = 2\pi R^2 \ell c \cdot \frac{\tau_m^n}{n+2}$$

The maximum elastic energy is found in similar fashion:

$$W = \int_0^R \frac{\tau^2}{2G} \cdot 2\pi\ell\rho d\rho = \frac{\pi R^2 \ell}{4G} \cdot \tau_m^2$$

Combining these expressions, we find that the specific damping capacity is:

$$\psi = \frac{8Gc}{n+2} \tau_m^{n-2} \qquad (17)$$

Equation 17 is plotted in dimensionless form in Figure 30 for values of n from 2 to 3. Comparison of these curves with the experimental results shows that the data cannot be described by a single relation of the form of Equation 17. Since the data appear to follow a law of the form

$$\psi = A + B\tau_m \qquad (18)$$

it is evident that two terms of the form of Equation 17 are necessary, one in which n is equal to 2 and one in which n is 3. It is proposed, therefore, that the energy dissipation is given by a law of the form

$$\Delta W = \alpha\tau^2 + \beta\tau^3 \qquad (19)$$

As a consequence of Equation 19, we have, corresponding to Equation 17:

$$\psi = 2G\alpha + \frac{8G}{5}\beta\tau_m \qquad (20)$$

From the correspondence between Equations 18 and 20, it is possible to compute the constants α and β in Equation 19.

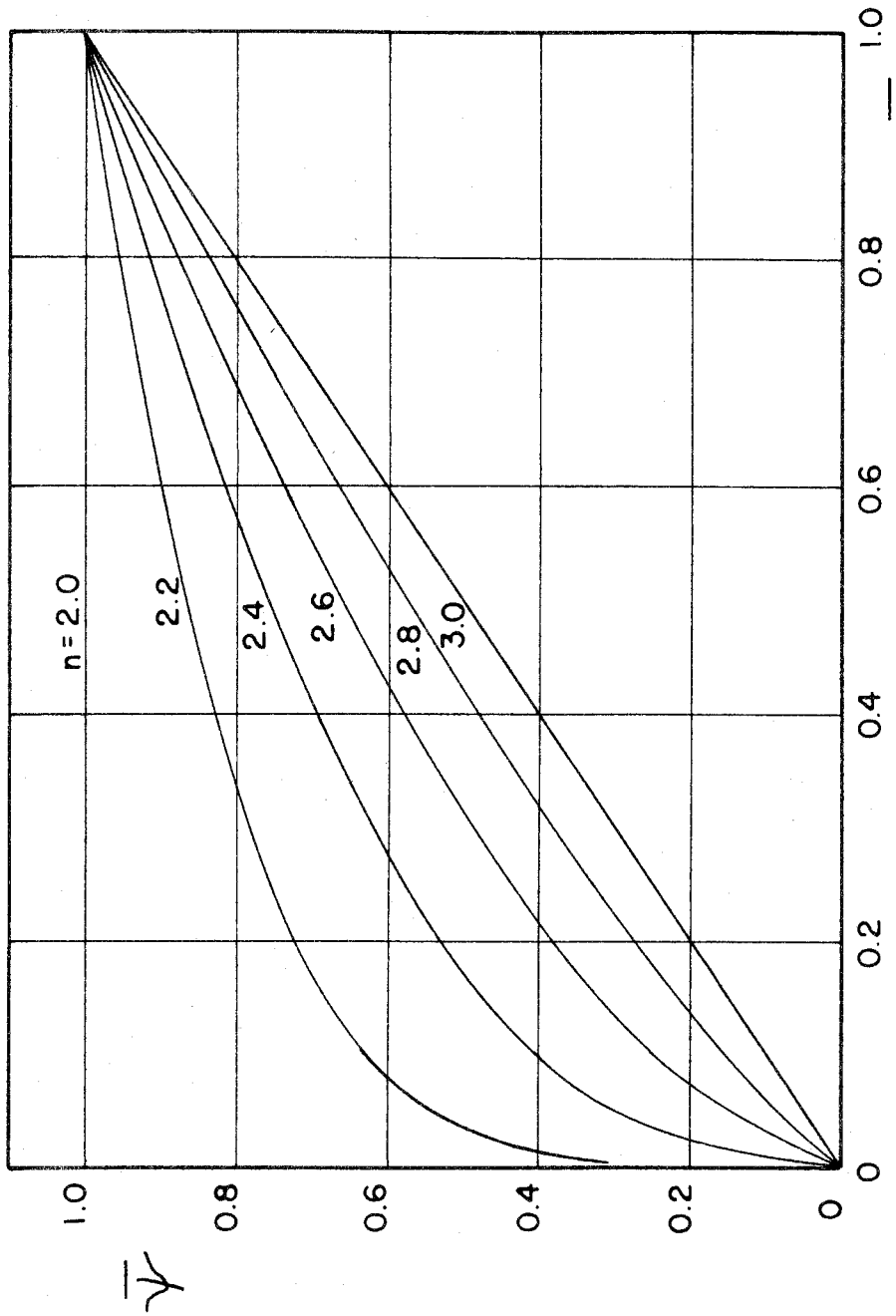

Figure 20. Dimensionless curves of specific damping capacity versus maximum shear stress

These values are given in Table IV for the SAE 1038 and SAE x-4130 steels.

It is noteworthy that the above relation is not a function of specimen size, but depends only upon the material constants and the maximum torsional stress.

TABLE IV

CALCULATED VALUES OF INTERNAL FRICTION CONSTANTS

Material	α	β
SAE 1022	8.7×10^{-11}	2.9×10^{-14}
SAE x-4130	1.2×10^{-11}	3.0×10^{-14}

If Equation 19 is a valid expression for the energy dissipation per unit volume per cycle, then it should be possible to calculate the specific damping capacity for a hollow specimen from the constants given in Table IV. Consider a hollow cylindrical specimen of outer radius R, Inner radius r, and length l, vibrating as in the experiments described above. The total energy dissipation is calculated by integrating Equation 19 over the volume of the specimen:

$$\Sigma(\Delta W) = \int_r^R (\alpha\tau^2+\beta\tau^3)\cdot 2\pi l\rho\, d\rho$$
$$= \pi R^2 l\left[\frac{\alpha}{2}\left(1-\frac{r^4}{R^4}\right)\tau_m^2 + \frac{2\beta}{5}\left(1-\frac{r^5}{R^5}\right)\tau_m^3\right]$$

The maximum elastic energy is:

$$W = \int_r^R \frac{\tau^2}{2G}\cdot 2\pi l\rho\, d\rho$$
$$= \pi R^2 l\left(1-\frac{r^4}{R^4}\right)\cdot\frac{\tau_m^2}{4G}$$

Combining the foregoing expressions, we obtain the specific damping capacity:

$$\psi = 2G\alpha + \frac{8G}{5}\beta\cdot\frac{1-(r/R)^5}{1-(r/R)^4}\cdot\tau_m \qquad (21)$$

The only difference between this expression and Equation 20 is in the slope; the intercept remains the same. The change in slope depends upon the ratio of inner to outer radius and is independent of the specimen size.

The hollow specimens tested had an outer radius of .125 inch and an inner radius of .094 inch.

$$r/R = .094/.125 = .75$$
$$\frac{1-(.75)^5}{1-(.75)^4} = 1.116$$

Accordingly we should expect the hollow torsional results to lie along a line having the same intercept but 12 percent greater slope than the solid torsional results. The

experimental results for solid and for hollow torsion specimens are compared in Figure 31.

In the comparison the predictions are confirmed to the extent that the intercepts agree within the uncertainty of the calculated values. The change in slope is minus 10 percent in one case and plus 40 percent in the other. Since the uncertainty involved in calculating the slope from data of the observed scatter is of the same order as the sought -- for change in slope, it appears that the normal errors inherent in the damping test are greater than the change of internal friction due to non-uniform stress distributions such as were obtained in the present experiments.

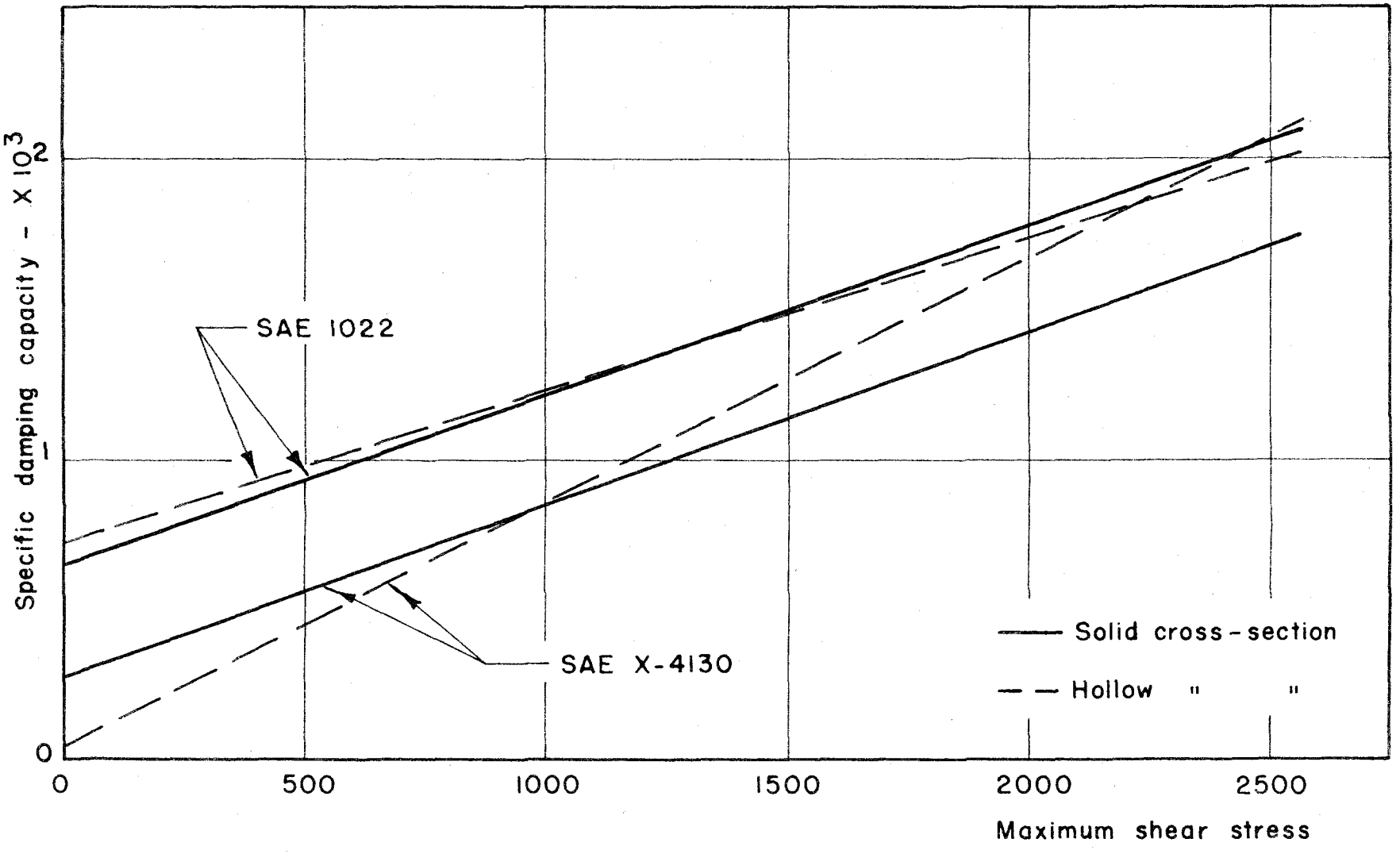

Figure 21. Comparison of torsional results

CONVERSION FROM SHEAR TO NORMAL STRESS

Modern theories (38) of the plastic properties of solids describe the basic process in plastic deformation as one of shearing. In speaking of energy dissipated by plastic action, therefore, shearing stress is regarded as fundamental. In order to calculate the specific damping capacity in practical situations, however, it would be desirable to have an expression for energy dissipation in terms of normal stress.

It is logical to assume that the energy dissipated by plastic action is proportional to the distortion of the crystal lattice and that, therefore, a normal stress amplitude which produced the same lattice distortion as a given shear stress amplitude would cause the same energy dissipation. The equivalence of normal and shear stress from the standpoint of distortion is given by the distortion strain energy theory (47) for the strength of materials. According to this theory the relation between shear and normal stress for equal distortion strain energy is

$$\tau = .577\,\sigma \qquad (33)$$

The assumption that energy dissipation is proportional to distortion strain energy is supported by the findings of Robertson and Yorgiadis (3), who reported that their data on energy dissipation in shear and in normal stress cycles could be reconciled by a relation such as Equation 33 in which the constant varied between .51 and .60 for steels.

Additional support for this theory is provided by the work of Bridgman (48), who found no plastic deformation after subjecting metals to intense hydrostatic pressures.

On the basis of Equation 22, we can rewrite Equation 19 in a form suitable for normal stress:

$$\Delta W = \alpha' \sigma^2 + \beta' \sigma^3 \tag{23}$$

in which

$$\alpha' = (.577)^2 \alpha = .333 \alpha$$
$$\beta' = (.577)^3 \beta = .192 \beta \tag{24}$$

CALCULATION OF SPECIFIC DAMPING CAPACITY IN BENDING

With the aid of Equation 33, it is possible to compute the specific damping capacity for a beam in bending vibration. In the following calculations, simple beam theory is used and the effect of transverse shearing force is neglected.

Consider a free-free beam, as shown in Figure 38, vibrating in its first symmetrical mode. The total energy dissipation may be found, in theory, by integrating Equation 33 over the volume of the beam:

$$\Sigma(\Delta w) = \int_v (\alpha'\sigma^2 + \beta'\sigma^3)\, dV \qquad (35)$$

The stress is given by

$$\sigma = \frac{M(x)\, y}{I}$$

and since

$$M(x) = EI\, \xi''(x)$$

we can express the variation of moment along the length of the beam in terms of the moment at the midpoint:

$$\frac{M(x)}{M(0)} = \frac{\xi''(x)}{\xi''(0)} = \frac{\bar{\xi}''(\bar{x})}{\bar{\xi}''(0)} = f(\bar{x}) \qquad (36)$$

in which the bars indicate the dimensionless form of the variables. Substituting these relations in Equation 35, the integral becomes

$$\Sigma(\Delta w) = 2\alpha' \left[\frac{M(0)}{I}\right]^2 \int_0^{\ell}\int_{-h/2}^{h/2}\int_{-b/2}^{b/2} f^2(\bar{x})\, y^2\, dx\, dy\, dz$$

$$+ 2\beta' \left[\frac{M(0)}{I}\right]^3 \int_0^{\ell}\int_{-h/2}^{h/2}\int_{-b/2}^{b/2} f^3(\bar{x})\, y^3\, dx\, dy\, dz$$

Performing the integrations and noting that $\frac{M(0)}{I} = \frac{2\sigma_m}{h}$,

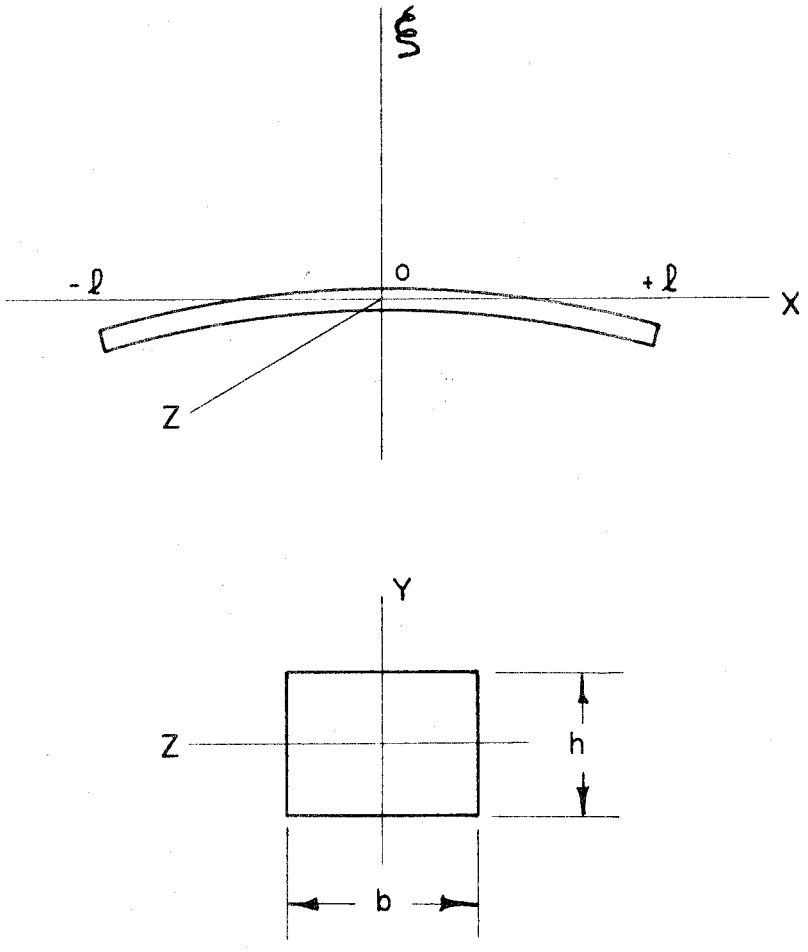

Figure 22. Sketch of a free-free beam

the integrals reduce to

$$\Sigma(\Delta W) = \alpha' \sigma_m^2 \frac{2bh\ell}{3} \int_0^1 f^2(\bar{x})\, d\bar{x} + \beta' \sigma_m^3 \frac{bh\ell}{2} \int_0^1 f^3(\bar{x})\, d\bar{x} \qquad (37)$$

The maximum elastic energy is given by

$$W = 2 \times \frac{1}{2EI} \int_0^\ell M^2(x)\, dx$$

With the aid of the above relations this expression reduces to:

$$W = \sigma_m^2 \frac{bh\ell}{3E} \int_0^1 f^2(\bar{x})\, d\bar{x} \qquad (38)$$

The specific damping capacity is then

$$\psi = 2E\alpha' + \frac{3E}{2}\beta' \frac{\int_0^1 f^3(\bar{x})\, d\bar{x}}{\int_0^1 f^2(\bar{x})\, d\bar{x}} \sigma_m \qquad (39)$$

Dimensionless tables of the beam curvatures appearing in Equation 26 are available (49), from which the ratio in the second term of Equation 29 is evaluated in Table V by application of Simpson's Rule. Using the calculated value of this ratio and Equations 34, the specific damping capacity can be expressed in terms of the internal friction constants determined in the torsional tests:

$$\psi = .666E \times \alpha + 1.26E \times \beta \times \sigma_m \qquad (30)$$

It should be observed that this expression depends only upon the material constants and upon the maximum stress in the beam; it is implied that the beam is rectangular and that the distribution of normal stress is linear over the depth of the beam.

An attempt was made to test Equation 30 by means of experiments with free-free beams supported at their nodes

TABLE V

Evaluation of ratio appearing in Equation 29

1 $\bar{x}$	2 $\bar{y}_1''$	3 $f(\bar{x})$	4 $f^2(\bar{x})$	5 $f^3(\bar{x})$	6 N_s	7 $N_s f^2(\bar{x})$	8 $N_s f^3(\bar{x})$
.00	4.4517	1.0000	1.0000	1.0000	1	1.0000	1.0000
.05	4.4279	.9947	.9894	.9842	4	3.9576	3.9368
.10	4.3569	.9787	.9579	.9375	2	1.9158	1.8750
.15	4.2399	.9524	.9071	.8639	4	3.6284	3.4556
.20	4.0793	.9163	.8396	.7693	2	1.6792	1.5386
.25	3.8775	.8710	.7586	.6607	4	3.0344	2.6428
.30	3.6391	.8175	.6683	.5463	2	1.3366	1.0926
.35	3.3679	.7565	.5723	.4329	4	2.2892	1.7316
.40	3.1255	.7021	.4929	.3461	2	.9858	.6922
.45	2.7501	.6178	.3817	.2358	4	1.5268	.9432
.50	2.4158	.5427	.2945	.1598	2	.5890	.3196
.55	2.0732	.4657	.2169	.1010	4	.8676	.4040
.60	1.7307	.3888	.1512	.0588	2	.3024	.1176
.65	1.3956	.3135	.0983	.0308	4	.3932	.1232
.70	1.0768	.2419	.0585	.0142	2	.1170	.0284
.75	0.7817	.1756	.0308	.0054	4	.1232	.0216
.80	0.5202	.1169	.0137	.0016	2	.0274	.0032
.85	0.3005	.0675	.0046	.0003	4	.0184	.0012
.90	0.1331	.0299	.0009	.0000	2	.0018	.0000
.95	0.0232	.0052	.0000	.0000	4	.0000	.0000
1.00	0.0000	0.0000	0.0000	0.0000	1	0.0000	0.0000

$\Sigma_7 = 23.7938$ $\Sigma_8 = 19.9272$

$$\frac{\Sigma_7}{\Sigma_8} = \frac{19.9272}{23.7938} = .8375$$

on fine threads. Strain measurements were made with bonded-wire gages cemented to the beam at mid-length; the strain signals during vibration were amplified and displayed on a cathode-ray tube, from which they were recorded on 35-millimeter film. At the very low stress levels attained in these tests the errors inherent in the determination of specific damping capacity were sufficient to obscure the small changes predicted by the theory. The calculation is of value, however, in that it points out the smallness of the corrections to internal friction which are to be expected on the basis of non-uniform stress distributions.

Experimental data is available in the work of Schabtach and Fehr (41) on tuning forks, which approximate the vibration of an ideal cantilever beam. It is of interest, therefore, to calculate the specific damping capacity for a cantilever beam. The calculation proceeds as does that for the free-free beam with the exception that a new moment-distribution function, $g(\bar{x})$, is required. Equation 29 is thus replaced by:

$$\psi = 2E \times \alpha' + \frac{3E}{2} \times \beta' \times \frac{\int_0^1 g^3(\bar{x})\, d\bar{x}}{\int_0^1 g^2(\bar{x})\, d\bar{x}}\, \sigma_m \qquad (31)$$

The ratio of the integrals in Equation 31 is computed in Table VI. Substituting this ratio and Equations 24 into Equation 31, we have for the cantilever, in terms of the experimental torsion constants:

$$\psi = .666E \times \alpha + 1.11E \times \beta \times \sigma_m \qquad (32)$$

This relation is plotted in Figure 23, using the experimental

TABLE VI

Evaluation of Ratio appearing in Equation 31

1 $\bar{x}$	2 $\bar{y}_1''$	3 $g(\bar{x})$	4 $g^2(\bar{x})$	5 $g^3(\bar{x})$	6 N_S	7 $N_S g^2(\bar{x})$	8 $N_S g^3(\bar{x})$
.00	3.5156	1.0000	1.0000	1.0000	1	1.0000	1.0000
.05	3.2737	0.93119	0.86711	0.80745	4	3.4684	3.2298
.10	3.0320	0.86244	0.74380	0.64149	2	1.4876	1.2830
.15	2.7907	0.79380	0.63012	0.50019	4	2.5205	2.0008
.20	2.5507	0.72553	0.52639	0.38191	2	1.0528	0.7638
.25	2.3126	0.65781	0.43271	0.28464	4	1.7308	1.1386
.30	2.0775	0.59093	0.34920	0.20635	2	0.6984	0.4127
.35	1.8467	0.52528	0.27592	0.14494	4	1.1037	0.5798
.40	1.6215	0.46122	0.21272	0.09811	2	0.4254	0.1962
.45	1.4034	0.39919	0.15935	0.06361	4	0.6374	0.2544
.50	1.1940	0.33962	0.11534	0.03917	2	0.2307	0.0783
.55	0.9950	0.28302	0.08010	0.02267	4	0.3204	0.0907
.60	0.8086	0.23000	0.05290	0.01217	2	0.1058	0.0243
.65	0.6362	0.18096	0.03275	0.00593	4	0.1310	0.0237
.70	0.4803	0.13662	0.01867	0.00255	2	0.0373	0.0051
.75	0.3424	0.097394	0.00720	0.000533	4	0.0288	0.0021
.80	0.2251	0.064028	0.004100	0.000263	2	0.0082	0.0005
.85	0.1300	0.036978	0.001367	0.0000506	4	0.0055	0.0002
.90	0.0595	0.016925	0.000287	0.00004848	2	0.0006	0.0001
.95	0.0156	0.004437	0.0001969	0.000008735	4	0.0008	0.0000
1.00	0.0000	0.0000	0.0000	0.0000	1	0.0000	0.0000

$\Sigma_7 = 14.9941$ $\Sigma_8 = 11.0841$

$$\frac{\Sigma_8}{\Sigma_7} = 0.73923$$

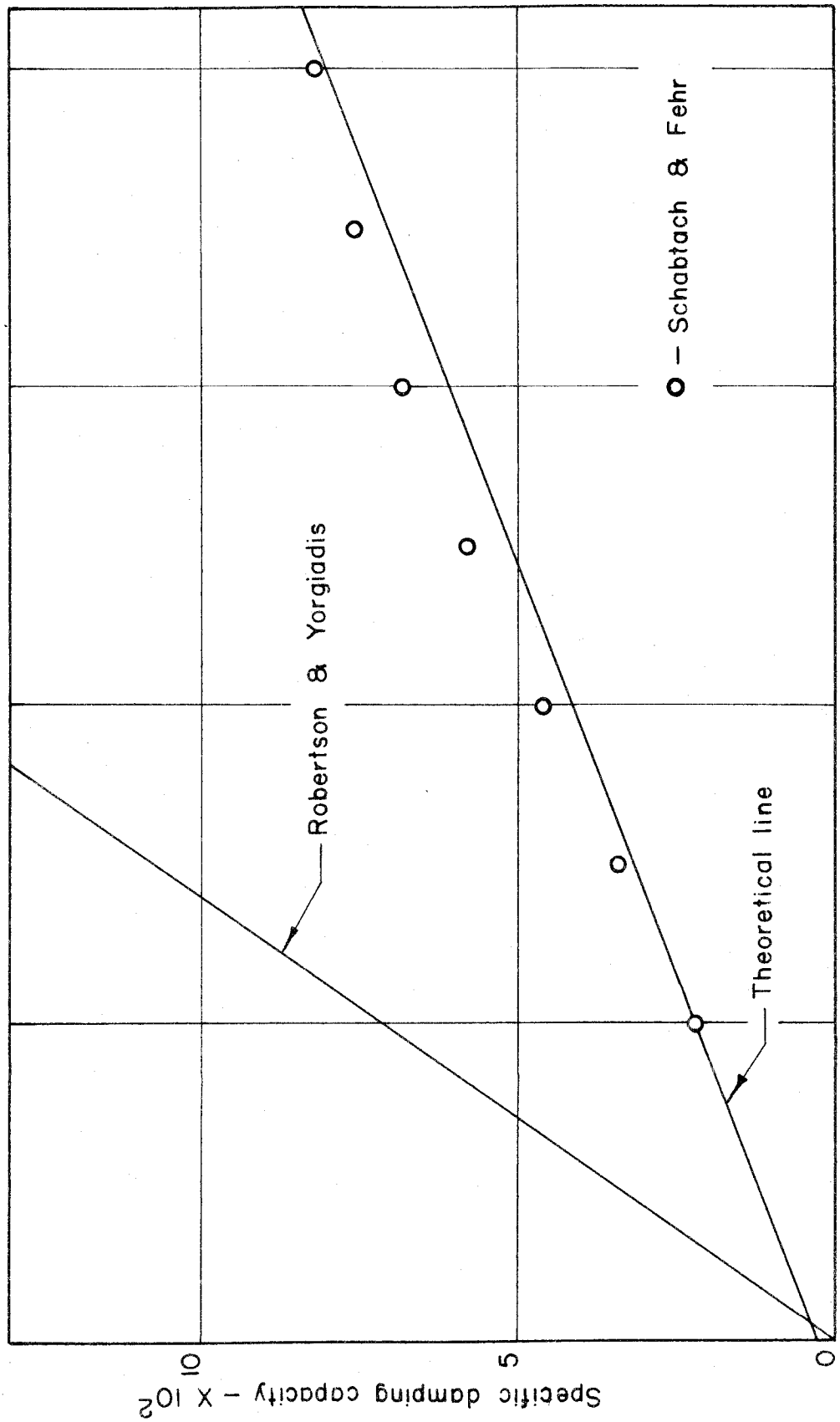

Figure 23. Comparison of theory with experiment for cantilever beam

values of α and β for SAE x-4130 steel. The small circles represent Schabtach and Fehr's data for SAE 4140 steel, a material of very similar composition and properties.

It was mentioned above that Robertson and Yorgiadis (3) proposed that energy dissipation is proportional to the cube of stress amplitude. If this theory be applied to the specific damping capacity of the cantilever beam, the result is a single term identical to the second term on the right-hand side of Equation 31. For purposes of comparison, such a line has been drawn through the origin in Figure 33, using the experimental value of β' given for SAE x-4130 steel by Robertson and Yorgiadis.

It is apparent from Figure 33 that the numerical value of β' given by Robertson and Yorgiadis is not consistent with the beam data of Schabtach and Fehr. The discrepancy is so great as to suggest that these investigators may have observed some phenomenon quite different from those considered in this study, particularly in view of the fact that the material which they used was of almost identical composition and condition as the materials used in this study and by Schabtach and Fehr. This wide disparity between the results of two modern investigations, conducted with careful attention to extraneous energy losses and calculation errors, is indicative of the state of knowledge of internal friction at high stress amplitudes.

The scale of Figure 33 does not permit a clear choice between a cubic law of energy dissipation on the one hand

and a square-plus-cubic law on the other. To choose between the two requires dependable data in the medium stress region; this data is provided by the experiments reported in this thesis. Furthermore, the bulk of the evidence cited in the Introduction is to the effect that the specific damping capacity does not approach zero as the stress amplitude approaches zero; This fact is accommodated by the square-plus-cubic hypothesis. Finally, the logical extension of the square-plus-cubic law, together with numerical values presented in this thesis, is seen to give a reasonably accurate preduction of the available data. It therefore seems reasonable to believe that the energy dissipation due to plastic effects is described by a law of the form

$$\Delta W = \alpha T^2 + \beta T^3 \qquad (19)$$

It should be added in reservation that the foregoing statement is based upon an observed linear variation of specific damping capacity in the medium stress range. The extent to which this condition may be satisfied in metals other than those studied is beyond the scope of this thesis.

DISCUSSION OF POROUS METAL RESULTS

Inspection of Figures 17, 18, and 19 shows that there is little consistency in the values of slope and intercept between lines representing supposedly identical materials. Nor is there a correlation between the differences of the mean lines and the minor differences of porosity within each group of specimens. This characteristic of the porous metals has been reported previously by the author (43); after radiographic examination of the specimens it was concluded that the differences could not be attributed to macroscopic defects within the material.

A more probable explanation is to be found in the structure-sensitivity of internal friction. The dotted lines for the alpha plus gamma region in Figure 24 indicate that the alloy of which the porous specimens were composed (20 percent nickel) is subject to a sluggish transformation at low temperatures. After rapid cooling the structure is martensitic; after very slow cooling it consists of alpha and gamma phases. Since the transformation involved is sluggish, variation of structure between individual specimens is to be expected. This variation of structure is a possible reason for the observed lack of agreement of internal friction for nominally identical porous metals.

No explanation is available for the difference between the results of successive tests on Specimen 13. Read (33) found that the internal friction of single crystals of zinc

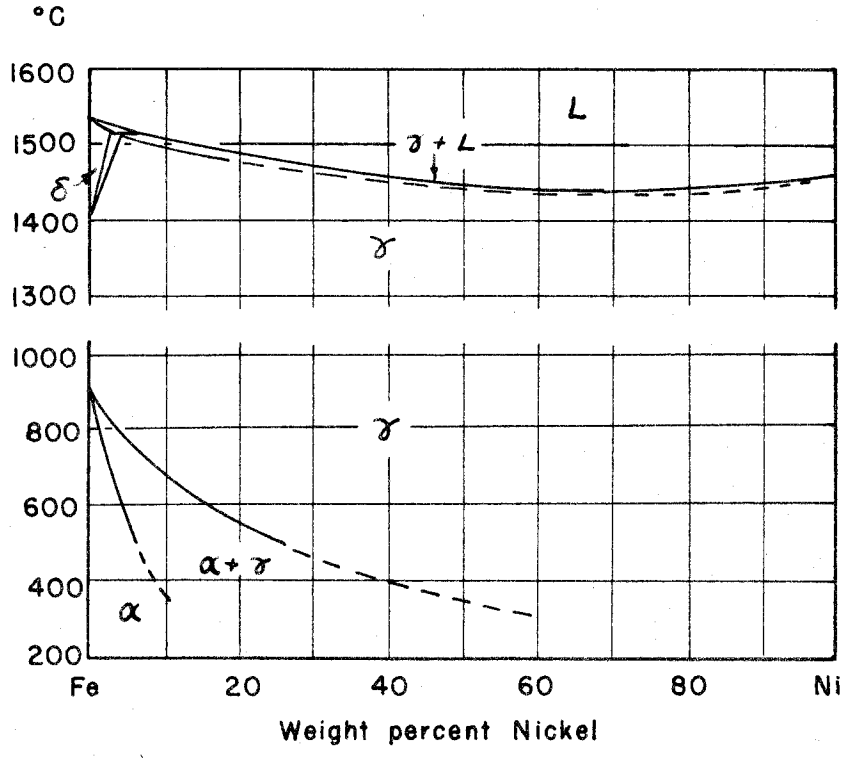

Figure 24. Equilibrium diagram for Iron–Nickel system (Sachs)

increased after vibration at large strain amplitudes; however, the increase was gradual and occurred after many more cycles than the few hundreds to which Specimen 13 was subjected in the first test. Hanstock (13) observed a change of internal friction in an aluminum alloy during continuous vibration. Here the change was associated with an induced precipitation-hardening and took place over 10^6 or more cycles. If the observed effect were due to a property of the porous metal or to a characteristic of the experimental apparatus, more than one occurrence would be expected since each porous metal specimen was subjected to two or more tests. It was therefore concluded that the effect was an abnormal one and that it does not alter the general nature of the results.

The measured values of specific damping capacity for porous nickel-iron are not abnormally higher than those for the solid iron alloys studied in this investigation. Solid nickel-iron specimens were not available for comparison. Part of the difference may be accounted for by considering the fact that the stress customarily used in connection with porous metals is an apparent stress, computed as if the porous metal were a continuous, isotropic solid. Actually the material contains many pores of irregular size and shape and the true stress is much higher than the apparent stress. Consequently, if the solid metal of which the porous specimen is composed behaves as did the solid metals tested, the internal friction will be increased as a result of the higher stress level. The detailed analysis of the microscopic distribution of stress in the porous metal is beyond the scope of this study.

On the basis of the above reasoning and because, in general, the internal friction of the porous metals appears to follow the same type of law as does that of the solid metals tested, it is concluded that no special mechanisms of energy dissipation are active in the porous metal.

V. SUMMARY AND CONCLUSIONS

The results of this investigation may be summarized as follows:

1. A comprehensive review of the literature on internal friction is presented, with particular emphasis on contributions within the last decade. This review indicates that there are a number of mechanisms which contribute to internal friction and that the relative importance of these mechanisms changes with frequency of vibration, with temperature, and with type and magnitude of stress. These facts explain in part the lack of agreement in the experimental data available in the literature. It is concluded that most of the mechanisms of internal friction are not important for purposes of engineering design at the usual design stresses.

2. Experimental evidence is presented which indicates that, for three materials and within a range of 500-4000 lbs/in^2 maximum shearing stress, the specific damping capacity in torsional vibration is given by an expression of the form:

$$\psi = A + B\,T_{max}$$

3. Calculations are presented on the effect of non-uniform stress distribution on specific damping capacity for several forms of specimen, in a form suitable for comparison with experiment. It is shown that the specific

damping capacity does not vary markedly with non-uniformity of stress distribution because it is the quotient of two quantities which vary with stress amplitude in similar fashion. The differences in specific damping capacity predicted by the theory were so small that they were obscured by the errors inherent in the damping determination at the low stress attained in careful experiments on torsional specimens of hollow cross-section and on free-free beams.

4. The specific damping capacity for a cantilever beam is calculated from the experimental data on torsional vibration and the calculated result is shown to be in agreement with beam data from the literature.

5. As a result of the experimental measurements and the calculations, it is proposed that the energy dissipation per unit volume per cycle in a metal vibrating at high stress amplitudes is given by an expression of the form:

$$\Delta W = \alpha \tau^2 + \beta \tau^3$$

6. Experimental results are presented on the specific damping capacity of a porous metal and the reasons for wide variation therein are discussed.

APPENDIX A: DERIVATION OF THE VARIATION OF ANELASTIC INTERNAL FRICTION WITH FREQUENCY

The model of the visco-elastic solid described in the Introduction is reproduced below with the addition of a coordinate system

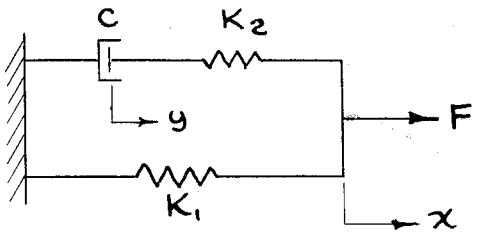

The equations of motion are:

$$\begin{aligned} F - K_1 x - K_2 (x-y) &= 0 \\ K_2 (x-y) - c\dot{y} &= 0 \end{aligned} \qquad (A)$$

Eliminating y from these equations, we obtain:

$$F + \frac{c}{K_2}\dot{F} = K_1 x + c\,\frac{K_1+K_2}{K_2}\,\dot{x} \qquad (B)$$

Equation B can be written in the form:

$$F + \tau_e \dot{F} = M_R (x + \tau_\sigma \dot{x}) \qquad (C)$$

using the notation

$\tau_e = \frac{c}{K_2}$, relaxation time at constant strain

$\tau_\sigma = \frac{c}{K_2} \times \frac{K_1+K_2}{K_1}$, " " " " stress

$M_R = K_1$, the relaxed modulus

$M_U = K_1 + K_2$, the un- " "

It is seen that

$$\frac{\tau_\sigma}{\tau_e} = \frac{M_U}{M_R} \qquad (D)$$

Equation D is identical with Equation 50 of Zener's monograph (33).

To investigate the internal friction, we let:

$$F = F_o\, e^{i\omega t}$$
$$x = x_o\, e^{i\omega t} \qquad (E)$$

Substituting Equations E in Equation C, we obtain, after simplifying:

$$F_o = \mathcal{M}\, x_o \qquad (F)$$

in which

$$\mathcal{M} = M_R \frac{1 + i\omega\tau_\sigma}{1 + i\omega\tau_e}$$, the complex modulus

A convenient measure of internal friction is the tangent of the angle by which strain lags stress, which tangent is given by the ratio of the imaginary and real parts of the complex modulus.

$$\tan\alpha = \frac{\omega(\tau_\sigma - \tau_e)}{1 + \omega^2\tau_\sigma\tau_e} \qquad (G)$$

Using $\bar{M} = (M_U M_R)^{1/2}$ and $\bar{\tau} = (\tau_\sigma\tau_e)^{1/2}$ for simplicity, Equation G appears in the form:

$$\tan\alpha = \frac{M_U - M_R}{\bar{M}} \times \frac{\omega\bar{\tau}}{1 + (\omega\bar{\tau})^2} \qquad (H)$$

The variation of tan α with the dimensionless product $\omega\bar{\tau}$ is depicted in Figure 5.

REFERENCES

(1) B. Hopkinson and G. T. Williams, "The Elastic Hysteresis of Steel", Proceedings, Roy. Soc. of London (1912), Ser. A, Vol. 87, p. 502.

(2) D. E. Hudson, "Internal Friction in Metals", thesis, California Institute of Technology (1942).

(3) J. M. Robertson and A. J. Yorgiadis, "Internal Friction in Engineering Materials", Transactions, Am. Soc. Mechanical Engrs., Journal of Applied Mechanics (1946), Vol. 13, No. 3, p. A-173.

(4) Committee for the Study of Viscosity of the Academy of Sciences at Amsterdam, "First Report on Viscosity and Plasticity", 2nd Edition, Amsterdam, 1939.

(5) C. M. Zener, "Anelasticity of Metals", Transactions Am. Inst. Mining and Metallurgical Engrs. (1946) Vol. 167, p. 155.

(6) Lord Kelvin (Sir Wm. Thompson), "On the Elasticity and Viscosity of Metals", Proceedings, Roy. Soc. of London (1865), Ser. A, Vol. 14, p. 289.

REFERENCES (continued)

(7) F. E. Rowett, "Elastic Hysteresis in Steel", Proceedings, Roy. Soc. of London (1914), Ser. A, Vol. 89, p. 528.

(8) O. Föppl, "The Practical Importance of the Damping Capacity of Metals, Especially Steels", Journal Iron and Steel Inst. (1936), Vol. 134, p. 393.

(9) L. Frommer and A. Murray, "Damping Capacity at Low Stresses in Light Alloys and Carbon Steel with Some Examples of Nondestructive Testing", Journal Inst. of Metals (1944), Vol. 70, p. 1.

(10) T. A. Read, S. W. Kitchen, and H. I. Fusfeld, "A Damping Test for Season Cracks in Cartridge Brass", Symposium on Stress-Corrosion Cracking, Am. Soc. Testing Materials, 1944.

(11) C. M. Zener, R. H. Randall, and F. C. Rose, "Intercrystalline Thermal Currents as a Source of Internal Friction", Phys. Rev. (1939), Vol. 56, p. 343.

(13) J. L. Snoek, "Effect of Small Quantities of Carbon and Nitrogen on the Elastic and Plastic Properties of Iron", Physica (1941), Vol. 8, p. 711.

REFERENCES (continued)

(13) R. F. Hanstock, "The Effect of Vibration on a Precipitation-Hardening Aluminum Alloy", Journal Inst. of Metals (1948), Vol. 74, p. 469.

(14) T. S. Kê, "High Temperature Anelastic Effects in Polycrystalline Aluminum", Phys. Rev. (1946), Vol. 70, p. 105.

(15) T. S. Kê, "Experimental Evidence of the Viscous Behavior of Grain Boundaries in Metals", Phys. Rev. (1947), Vol. 71, p. 533.

(16) T. S. Kê, "Stress Relaxation Across Grain Boundaries", Phys. Rev. (1947), Vol. 72, p. 72.

(17) T. S. Kê, "A Grain Boundary Model and the Mechanism of Viscous Intercrystalline Slip", Journal Appl. Phys. (1949), Vol. 20, No. 3, p. 274.

(18) A. L. Kimball, "Friction and Damping in Vibrations", Transactions, Am. Soc. Mechanical Engrs., Journal of Applied Mechanics (1941), Vol. 8, No. 1, p. A-37 and Vol. 8, No. 3, p. A-135.

REFERENCES (continued)

(19) E. V. Potter, "Damping Capacity of Metals", Report of Investigation 4194, U. S. Bureau of Mines (1948).

(20) W. L. Everitt, "Communication Engineering", McGraw-Hill Book Co., Inc., New York (1937), p. 65.

(21) B. J. Lazan, "Some Mechanical Properties of Plastics and Metals Under Sustained Vibration", Transactions, Am. Soc. Mechanical Engrs. (1943), Vol. 65, p. 87.

(22) G. A. Cottell, K. M. Entwistle, and F. C. Thompson, "The Measurement of the Damping Capacity of Metals in Torsional Vibration", Journal Inst. of Metals (1948), Vol. 74, p. 373.

(23) C. M. Zener, "Elasticity and Anelasticity of Metals", Univ. of Chicago Press (1948).

(24) K. Bennewitz and H. Rötger, "Über Die Innere Reibung Fester Korper; Absorptions Frequenzen Von Metallen in Akustichen Gebiet", Physik. Zeits. (1936), Vol. 37, p. 578.

REFERENCES (continued)

(35) C. M. Zener, W. Otis, and R. Nuckolls, "Internal Friction in Solids III - Experimental Determination of Thermoelastic Internal Friction", Phys. Rev. (1938), Vol. 53, p. 100.

(36) C. M. Zener, "Internal Friction in Solids II - General Theory of Thermoelastic Internal Friction", Phys. Rev. (1938), Vol. 53, p. 90.

(37) K. M. Entwistle, "The Effect of Grain Size on the Damping Capacity of Alpha Brass", Journal Inst. of Metals (1949), Vol. 75, p. 97.

(38) W. S. Gorsky, "On The Transitions in the Cu-An Alloy", Phys. Zeits. Sow. (1936), Vol. 6, p. 77.

(39) W. F. Brown, "The Variation of the Internal Friction and Elastic Constants with Magnetization in Iron", Phys. Rev. (1936), Vol. 50, p. 1165.

(30) D. Hanson and M. A. Wheeler, "The Deformation of Metals Under Prolonged Loading", Journal Inst. of Metals (1931), Vol. 45, p. 339.

REFERENCES (continued)

(31) H. Moore, B. Betty, and C. Dollins, "The Creep and Fracture of Lead and Lead Alloys", Univ. of Illinois Bull. No. 272, 1935.

(32) T. A. Read, "Internal Friction of Single Metal Crystals", Phys. Rev. (1940), Vol. 58, p. 371.

(33) T. A. Read, "Internal Friction of Single Crystals of Copper and Zinc", Transactions, Am. Inst. Mining and Metallurgical Engineers (1941), Vol. 143, p. 30.

(34) T. A. Read and E. P. T. Tyndall, "Internal Friction and Plastic Extension of Zinc Single Crystals", Journal Appl. Phys. (1946), Vol. 17, p. 713.

(35) C. M. Zener, D. Van Winkle, and H. Nielsen, "High-Temperature Internal Friction of Alpha Brass", Transactions, Am. Inst. Mining and Metallurgical Engrs. (1948), Vol. 147, p. 98.

(36) A. W. Lawson, "The Effect of Stress on Internal Friction in Polycrystalline Copper", Phys. Rev. (1941), Vol. 60, p. 330.

REFERENCES (continued)

(37) F. Swift and G. Richardson, "Internal Friction of Zinc Single Crystals", Journal Appl. Phys. (1947), Vol. 18, p. 417.

(38) F. Seitz and T. A. Read, "Theory of the Plastic Properties of Solids", Journal Appl. Phys. (1941), Vol. 12, pp. 100, 170, 470, 538.

(39) J. D. Eshelby, "Dislocations as a Cause of Mechanical Damping in Metals", Proceedings, Roy. Soc. of London (1949), Ser. A, Vol. 197, p. 396.

(40) G. P. Contractor and F. C. Thompson, "The Damping Capacity of Steel and Its Measurement", Journal Iron and Steel Inst. (1940), Vol. 138, p. 157.

(41) C. Schabtach and R. O. Fehr, "Measurement of the Damping of Engineering Materials During Flexural Vibration at Elevated Temperature," Transactions, Am. Soc. Mechanical Engrs., Journal of Applied Mechanics (1944), Vol. 11, No. 3, p. A-86.

(42) J. L. Alford, "Preliminary Investigation of the Damping Capacity of Porous Metals", Jet Propulsion Laboratory, California Institute of Technology (1948), Progress Report No. 4-52.

REFERENCES (continued)

(43) A. Gemant, "The Problem of the Reduction of Vibrations by the Use of Materials of High Damping Capacity", Journal Appl. Phys. (1944), Vol. 15, p. 33.

(44) J. Marin and F. B. Stulen, "A New Fatigue Strength - Damping Criterion for the Design of Resonant Members", Transaction, Am. Soc. Mechanical Engrs., Journal of Applied Mechanics (1947), Vol. 14, No. 3, p. A-309.

(45) A. L. Kimball and D. E. Lovell, "Internal Friction in Solids", Phys. Rev. (1927), Vol. 30, p. 948.

(46) F. M. Lewis, "Torsional Vibration in the Diesel Engine", Transactions, Soc. Naval Architects and Marine Engrs. (1935), Vol. 33, p. 104.

(47) S. P. Timoshenko, "Theory of Elasticity", McGraw-Hill Book Co., Inc., New York (1934).

(48) D. W. Bridgman, "The Physics of High Pressure", MacMillan Book Co., New York (1931).

(49) D. R. Branchflower, "Uniform Beam Deflection Tables", Northrop Aircraft Report STR-31, 1949.